

IV. MEDIUM-ENERGY NUCLEAR PHYSICS RESEARCH

OVERVIEW

The overall goals of the Medium-Energy Physics research program in the Argonne Physics Division are to test our understanding of the structure of hadrons and the structure of nuclei, and to develop and exploit new technologies for high-impact applications in nuclear physics as well as other national priorities. In order to test our understanding of the structure of hadrons and the structure of nuclei within the framework of quantum chromodynamics, the medium-energy research program emphasizes the study of nucleons and nuclei on a relatively short distance scale. Because the electromagnetic interaction provides an accurate, well-understood probe of these phenomena, primary emphasis is placed on experiments involving electron scattering, real photons and Drell-Yan processes. The electron beams of the Thomas Jefferson National Accelerator Facility (JLab) are ideally suited for studies of nuclei at hadronic scales and represent one center of the experimental program. Staff members led in the construction of experimental facilities, served as spokespersons or co-spokespersons for 20 experiments and were actively involved in others. The group constructed the general-purpose Short Orbit Spectrometer (SOS) which forms half of the coincidence spectrometer pair that is the base experimental equipment in Hall C. Last year, Argonne had a major role in re-establishing the SOS in Hall C for a series of five experiments. Argonne led the first experiment to be carried out at JLab in Fiscal Year 1996 and has completed 15 other experiments.

Recently, staff members have focused increasingly on studies of the nucleon and the search for exotic phenomena. In Fiscal Year 2004 the analysis was completed for the ratio of the electromagnetic elastic form factors of the proton using a modified Rosenbluth method. These results agree with data recorded previously with the traditional Rosenbluth method, but strongly disagree with the polarization transfer data. A new initiative to search for color transparency in ρ production in nuclei was completed last year in Hall B at JLab. This work represents an important extension of Argonne's earlier ρ electro-production studies at HERMES. A new experiment to search for partners of the Θ^+ pentaquark was completed last year in Hall A. Finally, two experiments, a study of the EMC effect in light nuclei and $x > 1$ studies in nuclei, were completed last year in Hall C. Three new proposals – a high-resolution search for the

Θ^+ pentaquark, a search for two-photon exchange effects in elastic electron-proton scattering, and parity-violating deep inelastic scattering from the deuteron – were approved this year by the JLab PAC.

The HERMES collaboration is studying the spin structure of the nucleon using internal polarized targets in the HERA storage ring at DESY. Deep inelastic scattering has been measured with polarized electrons on polarized hydrogen, deuterium and ^3He . Argonne has concentrated on the hadron particle identification of HERMES, a unique capability compared to other spin structure experiments. In 1999 and under Argonne leadership, the dual-radiator ring imaging Cerenkov counter (RICH) was brought into operation at the design specifications to provide complete hadron identification in the experiment. The RICH has been operating routinely since its installation. This has allowed HERMES to make decisive measurements of the flavor dependence of the spin distributions. Last year, HERMES met one of its principal objectives by publishing a five-component decomposition of the proton's spin structure function and the first measurement of the x-dependence of the strange sea polarization. During 2001, HERMES installed a transversely polarized target. Measurements with this target will continue through 2005. These results are expected to provide significant information on the quark's transverse motion. Finally, HERMES will continue the investigation of quark propagation in nuclear matter.


Measurements of high mass virtual photon production in high-energy proton-induced reactions have determined the flavor dependence of the sea of antiquarks in the nucleon. These measurements gave insight into the origin of the nucleon sea. In the same experiment, the high-x absolute Drell-Yan cross sections were measured. In Fiscal Year 2001, a new initiative was approved by the FNAL PAC to continue these measurements with much higher luminosity at the FNAL Main Injector. These Drell-Yan experiments not only provide the best means to measure anti-quark distributions in the nucleon and nuclei, but represent an outstanding opportunity to perform these measurements at an ideal proton beam energy of 120 GeV. Plans are underway to prepare this experiment at FNAL.

The technology of laser atom traps provides a unique environment for the study of nuclear and atomic systems and represents a powerful new method that is opening up exciting new opportunities in a variety of fields, including nuclear physics. In particular, the group has developed a high-efficiency, high-sensitivity magneto-optical trap for rare, unstable isotopes of krypton. Last year, the group demonstrated the power of this novel method by dating ancient Sarahan ground water. A highlight during this year was the optical trapping of single atoms of ^6He and performing precision laser spectroscopy on the individual ^6He atoms. The nuclear charge radius of ^6He was determined for the first time.

A new initiative to search for an electric dipole moment (EDM) of ^{225}Ra is in progress. The ultimate goal is to search for a non-zero EDM for ^{225}Ra and

improve the sensitivity for nuclear EDM searches by approximately two orders of magnitude. This test of time-reversal symmetry represents an outstanding opportunity to search for new physics beyond the Standard Model. Laser spectroscopy was performed for the ^{225}Ra beam from the oven system. A Zeeman slower and optical trap for ^{225}Ra are being developed.

A new experiment to measure parity violation in deep inelastic scattering from the deuteron was approved by the JLab PAC. The ultimate goal of this experiment is to provide the best possible measurement for the neutral current axial vector coupling to the quarks. Finally, as a test of one of the main assumptions underlying the NuTeV anomaly, a feasibility study is underway for a possible charge symmetry violation experiment at the partonic level.



A. HADRON PROPERTIES

a.1. New Measurement of (G_E/G_M) for the Proton (J. Arrington, R. Beams, K. Hafidi, R. J. Holt, I. A. Qattan, E. C. Schulte, K. Wijesooriya, X. Zheng, B. Zeidman, and the JLab E01-001 Collaboration)

The discrepancy between Rosenbluth and polarization transfer measurements of the proton electromagnetic form factors led to significant questions about our level of understanding of the proton. Experiment E01-001 was designed to provide a Rosenbluth measurement with both significantly improved sensitivity and greatly reduced systematic uncertainties than previous Rosenbluth measurements, to provide a definitive test of the consistency of the two techniques. The elastic cross section was measured by detecting the struck proton, rather than the scattered electron. This has several important advantages: (1) no ε -dependence to the momentum of the detected proton at fixed Q^2 , (2) much smaller ε -dependence to the measured cross section, (3) larger cross sections at low ε values, and (4) reduced size and ε -dependence of the radiative corrections.

The experiment ran at JLab in May 2002, and the extraction of the form factors is complete.¹ Figure IV-1 shows the extracted values of $\mu_p G_E/G_M$ compared to previous Rosenbluth and polarization transfer results. The new results disagree with the polarization transfer measurements, but are in excellent agreement with the previous Rosenbluth extraction. This rules out most possible explanations of the discrepancy in terms of experimental systematic errors, and also sets significant constraints on any possible error in the radiative corrections related to the scattered electron (which is not detected in this experiment). At this point, it would appear that the discrepancy between these two techniques must be a result of either a systematic error in the polarization transfer measurements, which have all been performed with the same spectrometer and polarimeter, or the result of an unknown physics correction to one or both techniques.

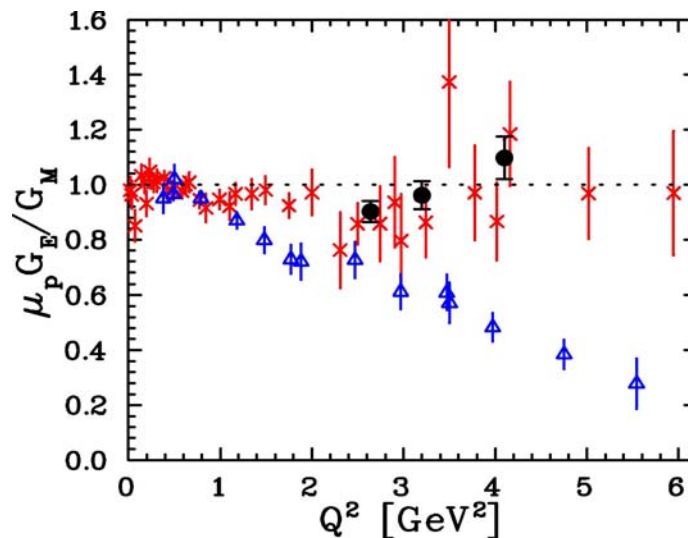


Fig. IV-1. Extracted values of $\mu_p G_E/G_M$ from E01-001¹ (solid circles), a global analysis of previous cross section measurements⁹ (red crosses), and JLab polarization transfer measurements (blue triangles).¹⁰

It is presently believed that two-photon exchange corrections are probably responsible for the discrepancy. While present efforts to calculate effect of two-photon exchange are not yet able to resolve the discrepancy, they do indicate that the effects are large enough to have a significant effect on the Rosenbluth extractions of the form factors. We are

involved in several experiments designed to test the hypothesis that two-photon exchange is responsible for the discrepancy, and if so, to extract the ε and Q^2 dependence of these corrections on both the cross section and polarization data. First, there are experiments that will test the systematic uncertainties of the polarization transfer data by making measurements with a different

spectrometer and polarimeter² or using a polarized target rather than a recoil polarimeter.³ A more direct test will be the comparison of positron-proton to electron-proton scattering, which is sensitive to two-photon exchange corrections. There is some evidence for two-photon corrections at large scattering angle from previous measurements,⁴ and

we have experiments planned to make improved positron-electron comparisons.^{5,6} Finally, there are experiments at JLab that will make precise measurements of the ε dependence of the polarization transfer⁷ and unpolarized cross section⁸ with enough sensitivity to measure or strongly constrain the effects of two-photon exchange.

¹I. A. Qattan *et al.*, Phys. Rev. Lett. **94**, 142301 (2005).

²JLab experiment E04-108, "Measurement of G_{Ep}/G_{Mp} to $Q^2 = 9 \text{ GeV}^2$ Via Recoil Polarization", C. F. Perdrisat, V. Punjabi, M. K. Jones, and E. Brash, spokespersons.

³JLab proposal PR04-111, "Measurements of G_{Ep}/G_{Mp} Using Elastic Polarized $\bar{p}(\bar{e}, e')p$ Up to $Q^2 = 5.6 \text{ (GeV/c)}^2$ ", X. Zheng, J. R. Calarco, and O. A. Rondan, spokespersons.

⁴J. Arrington, Phys. Rev. C **69**, 032201(R) (2004).

⁵VEPP-3 experiment, "Two-Photon Exchange and Elastic Scattering of Electrons/Positrons On the Proton", J. Arrington and D. M. Nikolenko, spokespersons.

⁶JLab experiment E06-116, "Beyond the Born Approximation: A Precise Comparison of Positron-Proton and Electron-Proton Elastic Scattering in CLAS", A. Afanasev, J. Arrington, W. K. Brooks, K. Joo, B. A. Raue, and L. B. Weinstein, spokespersons.

⁷JLab experiment E04-019, "Measurement of the Two-Photon Exchange Contribution in ep Elastic Scattering Using Recoil Polarization", R. Suleiman, L. Pentchev, C. F. Perdrisat, and R. Gilman, spokespersons.

⁸JLab experiment E05-017, "A Measurement of Two-Photon Exchange in Unpolarized Elastic Electron-Proton Scattering", J. Arrington, spokesperson.

⁹J. Arrington *et al.*, Phys. Rev. C **71**, 015202 (2005).

¹⁰M. K. Jones *et al.*, Phys. Rev. Lett. **84**, 1398 (2000); O. Gayou *et al.*, Phys. Rev. Lett. **88**, 092301 (2002).

a.2. High-Resolution Search for the Θ^+ Pentaquark at Jlab (P. E. Reimer, J. Arrington, K. Hafidi, R. J. Holt, D. H. Potterveld, E. C. Schulte, X. Zheng, and the E05-009 Collaboration)

Quantum Chromodynamics (QCD) governs the way in which quarks and gluons are bound into hadrons. Until recently, only two different configurations of quarks and antiquarks have been observed: mesons ($\bar{q}q$) and baryons (qqq). These are not the only configurations which can satisfy the basic QCD requirement that hadronic matter is color-neutral—many other configurations exist that also satisfy this condition. One example is the pentaquark ($qqqq\bar{q}$) configuration. Recently, experimental evidence and theoretical work have strongly suggested the existence of a pentaquark state, known as the Θ^+ with a mass near 1540 MeV. Experiment 05-009¹ at JLab will definitively establish or dismiss the existence of the Θ^+ pentaquark. If the Θ^+ exists, the experiment will determine its mass and measure its width.

The experiment will observe the decay products of the Θ^+ in the reactions ${}^2\text{H}(e, K^+K^+n)e'$ and ${}^2\text{H}(e, e'K^+n)K^-$. The K^+ and the neutron will be detected in the BigBite spectrometer and a large, high

resolution neutron detector, respectively. The invariant mass of the K^+n system will be reconstructed to search for the Θ^+ . The remaining kaon or electron will be detected in the HRS spectrometer as a tag on the event. Because of space limitations between the detectors and the beamline, both BigBite and the neutron array will be located out-of-plane. The expected instrumental resolution on the invariant mass is 2.1 MeV (FWHM) and the mass will be established with an absolute accuracy of 0.5 MeV. Based on existing data from Spring-8, the photoproduction cross-section of the Θ^+ is expected to be at least 1.6 nb. Even for a cross-section this small, the Θ^+ could be observed in this experiment with a signal that is seven times that of the statistical fluctuations.

This experiment was approved in early 2005 and current efforts are focused on optimizing the design and constructing the BigBite spectrometer detector package. The experiment could be ready to collect data in late 2007.

¹J. P. Chen *et al.*, "High Resolution Study of the Resonance in nK^+ System", proposal 05-009 to the JLab PAC, G. Cates, P. E. Reimer, B. Wojtsekhowski, spokespersons, December 6, 2004.

a.3. Search for Additional Pentaquark States at Jlab (P. E. Reimer, J. Arrington, K. Hafidi, E. C. Schulte, X. Zheng, and the E04-012 Collaboration)

All observed hadrons have fallen into two categories, mesons made of a quark-antiquark pair mesons ($\bar{q}q$) and baryons composed of three quarks (qqq). These are, however, not the only configurations of quarks and antiquarks allowed by the underlying theory, Quantum Chromodynamics. Configurations not fitting into the meson and baryon framework are known as "exotics". A possible exotic configuration is a pentaquark state with four quarks and an antiquark ($qqqq\bar{q}$). Recently, experimental evidence and theoretical work have suggested the existence of a pentaquark state, known as the Θ^+ with a mass near 1540 MeV. Within the Chiral Soliton model, this state is a member of a set of 10 pentaquark states known as an antidecuplet. Using Hall A at JLab, E04-012¹ was able to search for several antidecuplet-partner states to the Θ^+ . Specifically, the experiment searched for the Σ^0 member of the antidecuplet in the reaction $H(e,e'K^+)X$ and the N^0 in the reaction $H(e,e'\pi^+)X$, by reconstructing the missing mass of the

system. Although these states are not explicitly exotic, the discovery of a narrow state would be a valuable confirmation of the existence of an antidecuplet of states. In addition, the experiment searched for the exotic isospin partner state, Θ^{++} , in the $H(e,e'K^-)X$ reaction. Assuming the mass of the Θ^+ to be around 1540 MeV, the antidecuplet structure limits the possible masses of the partners. In addition, the reported narrowness of the Θ^+ leads implies the partner states are also likely to be narrow. The experiment used collected data in May and June, 2004, using the HRS spectrometers to detect the scattered electron and the K^+ , π^+ and K^- respectively. The mass ranges accessible to the experiment were $1530 < M(\Sigma^0) < 1820$ MeV, $1600 < M(N^0) < 1830$ MeV and $1500 < M(\Theta^{++}) < 1600$ MeV. Preliminary results show no evidence for any narrow resonances within the candidate regions. Ongoing efficiencies studies and better understanding of the background will allow for strict upper limits to be placed on the existence of these states.

¹J. P. Chen *et al.*, "High Resolution Study of the 1540 Exotic State," proposal 04012 to the JLab PAC, P. E. Reimer and B. Wojtsekhowski, spokespersons, December 2, 2003.

a.4. $N \rightarrow \Delta$ Transition Form Factors (J. Arrington, K. Hafidi, R. J. Holt, P. E. Reimer, E. C. Schulte, X. Zheng, and the JLab E01-002 Collaboration)

Measurements of the nucleon transition form factors provide additional information on the structure of the nucleon and nucleon excitations, which complement the measurements of the nucleon elastic form factors. Experiment E01-002 was performed in the spring of 2003 and measured electroproduction of the $\Delta(1232)$ and $S_{11}(1535)$ baryon resonances. The experiment is an extension of previous, lower energy electroproduction experiments¹ at JLab, and at the higher momentum transfers achieved in this experiment we can probe the transition to the high-energy region where perturbative QCD is expected to describe the reaction. Data were taken to separate

out the magnetic dipole (M1), electric dipole (E2), and Coulomb (C2) contributions to the $N \rightarrow \Delta$ transition. The data are currently under analysis.

These measurements will provide a stringent test of recent calculations.²⁻⁴ T.-S. H. Lee has done extensive work on a dynamical model for pion electroproduction in the Δ region.² A. Krassnigg and C. D. Roberts are exploring the effects of axial-vector diquark and pion cloud contributions to the nucleon elastic and $N \rightarrow \Delta$ transition form factors,³ while F. Coester has performed similar explorations of relativistic effects in the elastic and transition form factors.⁴

¹V. Frolov *et al.*, Phys. Rev. Lett **82**, 45 (1999); C. S. Armstrong *et al.*, Phys. Rev. D **60**, 052004 (1999).

²T. Sato and T.-S. H. Lee, Phys. Rev. C **63**, 055201 (2001); T. Sato, T.-S. H. Lee, and T. Nakamura, nucl-th/041182 (2004).

³R. Alkofer *et al.*, nucl-th/0412045 (2004).

⁴B. Julia-Diaz *et al.*, Phys. Rev. C **69**, 035212 (2004).

a.5. The Charged Pion Form Factor (J. Arrington, K. Hafidi, R. J. Holt, P. E. Reimer, E. C. Schulte, X. Zheng, and the JLab E01-004 Collaboration)

A complete understanding the structure of the nucleon is the defining problem in QCD. However, while experiments on the proton are relatively easy, the complicated structure of a three light-quark system makes modeling of the proton in realistic, QCD-based models, is difficult. The pion structure is simpler, and can in some cases provide a better meeting ground between theory and experiment in the study of QCD. Experiment E01-004 is an extension to the previous JLab measurement¹ of the pion form factor, and will improve measurements of

the form factor at 1.6 GeV^2 , the highest value at which the form factor has been measured, as well as extend measurements to 2.5 GeV^2 . These measurements can be used to test models of hadron structure in a simpler system than the nucleon, where more advanced calculations can be performed. The form factor provides information on spatial distribution of the pion constituents, complementary to the information on the quark momentum distributions from the pion structure function measurements. The experiment ran in the summer of 2003, and the analysis is underway.

¹J. Volmer *et al.*, Phys. Rev. Lett. **86**, 1713 (2001).

a.6. Separated and Unseparated Structure Functions in the Nucleon Resonance

Region (J. Arrington, D. Gaskell, D. F. Geesaman, K. Hafidi, R. J. Holt, B. A. Mueller, T. G. O'Neill, D. H. Potterveld, P. E. Reimer, E. C. Schulte, X. Zheng, and the E94-110, E00-002, E00-108, and E00-116 Collaborations)

At high energies, inclusive electron scattering provides a clean and direct probe of the quark distributions in nucleons. At low energies, this simple picture of electron-quark scattering is not valid and the scattering is better understood in terms of resonance excitations and pion production. Measurements of the unpolarized F_2 structure function show a smooth transition between the deep inelastic regime of quasifree quark scattering to the resonance excitation regions, and on average, the resonance region structure function reproduces the deep inelastic limit¹ when taken as a function of ξ . At large momentum transfer, ξ is equivalent to Bjorken- x and represents the momentum fraction of the struck quark. At lower momentum transfers, ξ takes into account scaling violations due to the finite target mass.

Additional measurements of the F_2 structure function of the proton and deuteron in the transition region were made at JLab to better study the phenomenon¹ of Local Duality. While the structure function does change at low Q^2 values, and resonance structure was

clearly visible, the total strength in the region of any of the prominent resonances is identical to the strength in the DIS region to better than 10% down to $Q^2 = 0.5 \text{ GeV}^2$. Furthermore, for very low ξ values, the structure function shows a valence-like behavior, becoming very small as ξ decreases. A more recent experiment, E94-110, extended these measurements by making a Rosenbluth separation of both F_1 and F_2 . These data provided the first observation of duality in both the longitudinal and transverse channels for the proton. They also provided the first indication of significant longitudinal contributions to resonance electroproduction. Final results have been obtained for the L-T separation of both the resonance region structure function³ (Fig. IV-2) and the elastic electron-proton cross sections.⁴ In 2003, three additional measurements were performed in Hall C to further investigate the nature of duality: E00-116, E02-002, and E00-108. Measurements of F_2 for both the proton and deuteron were extended to higher Q^2 values than in the initial investigations. Measurements of the separated structure functions, F_1 and F_2 , were performed at very low x and Q^2 , to investigate in more detail the valence-like nature of the resonance region structure

functions. Finally, these measurements were extended beyond inclusive scattering, to determine if a similar duality is observed in semi-inclusive scattering, where a single high-momentum pion is

tagged in the final state. These experiments were completed in the summer of 2003, and are the data are currently under analysis.

¹E. D. Bloom and F. J. Gilman, Phys. Rev. Lett. **25**, 1140 (1970).

²I. Niculescu *et al.*, Phys. Rev. Lett. **85**, 1182 (2000); *ibid.*, **85**, 1186 (2000).

³M. E. Christy *et al.*, Phys. Rev. C **70**, 015206 (2004).

⁴Y. Liang *et al.*, nucl-ex/0410027 (2004).

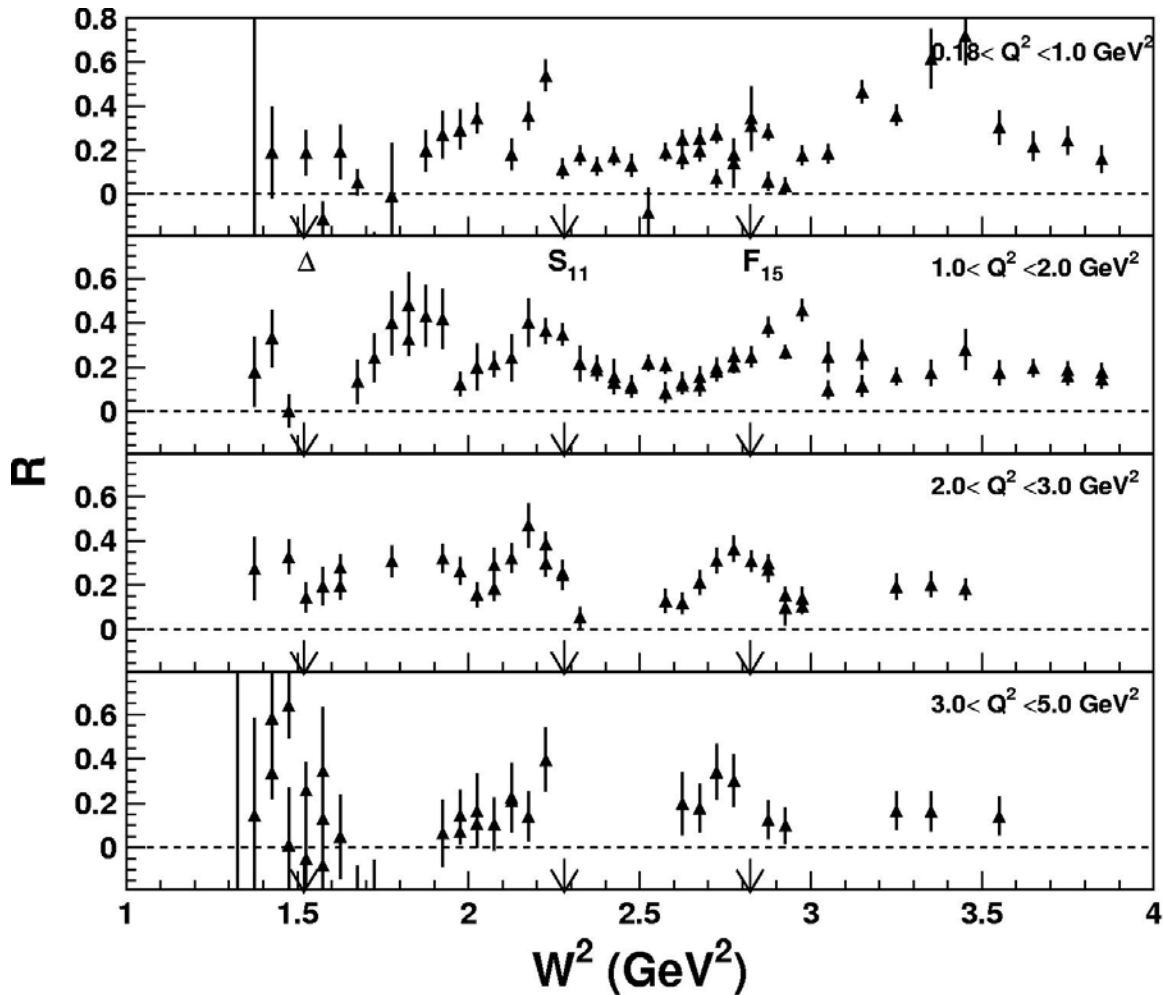


Fig. IV-2. Extracted value of $R = \sigma_L/\sigma_R$ as a function of W^2 for four different ranges in Q^2 . The arrows indicate the positions of the Δ , S_{11} , and F_{15} resonance regions.

B. HADRONS IN THE NUCLEAR MEDIUM

b.1. Search for the Onset of Color Transparency: JLab E02-110 Experiment

(K. Hafidi, B. Mustapha, J. Arrington, A. El Alaoui, L. El Fassi, D. F. Geesaman, R. J. Holt, D. H. Potterveld, P. E. Reimer, E. C. Schulte, X. Zheng, and Hall B Collaboration)

According to QCD, pointlike colorless systems, such as those produced in exclusive processes at high Q^2 have quite small transverse sizes. Therefore, they are expected to travel through nuclear matter experiencing very little attenuation. This phenomenon is known as color transparency (CT). An analogous mechanism is well known in QED: the interaction cross section of an electric dipole is proportional to its square size. As a result the cross section vanishes for objects with very small electric dipole moments. Since color is the charge of QCD, and by analogy to QED, the cross section of a color-neutral dipole, as formed by a pair of oppositely colored quarks for instance, is also predicted to vanish for small sized hadrons. Color transparency cannot be explained by Glauber theory and calls upon quark degrees of freedom. Earlier measurements were mainly focused on quasi-elastic hadronic (p,2p)¹ and leptonic (e,e'p)² scattering from nuclear targets. None of these experiments were able to produce evidence for CT up to $Q^2 \sim 8 \text{ GeV}^2$. The strongest evidence for CT so far comes from Fermilab experiment E791 on the A-dependence of coherent diffractive dissociation of 500 GeV/c pions into di-jets.³ A recent measurement performed by the HERMES collaboration using exclusive ρ^0 electroproduction from nitrogen adds further evidence for the existence of CT.⁴

The main goal of E02-110 experiment⁵ is to search for the onset of CT in the incoherent diffractive ρ^0 electro and photoproduction on deuterium, carbon

and copper. In this process (see Fig. IV-3), the virtual photon fluctuates into $q\bar{q}$ pair which travels through the nuclear medium evolving from its small initial state with a transverse size proportional to $1/Q$, to a "normal size" vector meson detected in the final state. Therefore, by increasing the value of Q^2 one can squeeze the size of the produced $q\bar{q}$ wave packet. The photon fluctuation can propagate over a distance which is known as the coherence length l_c . The coherence length can be estimated relying on the uncertainty principle and Lorentz time dilation as $l_c = 2\nu / (Q^2 + M_{q\bar{q}}^2)$, where ν is the energy of the virtual photon and $M_{q\bar{q}}$ is the mass of the $q\bar{q}$ pair dominated by the ρ^0 mass in the case of exclusive ρ^0 electroproduction. What is measured in the reaction is how transparent the nucleus appears to "small size" ρ^0 by taking the ratio of the nuclear per-nucleon (σ_A/A) to the free nucleon (σ_N) cross-sections, which is called nuclear transparency $T_A = \sigma_A/A\sigma_N$. Consequently, the signature of CT is an increase in the nuclear transparency T_A with increasing hardness (Q^2) of the reaction. Recent theoretical calculations by Kopeliovich *et al.*⁶ predicted an increase of more than 40% at $Q^2 \sim 4 \text{ GeV}^2$. However, one should be careful about other effects that can imitate this signal. Indeed, measurements by HERMES have shown that T_A increases when l_c varies from long to short compared to the size of the nucleus. This so-called coherence length effect can mock the signal of CT and should be under control to avoid confusing it with the CT effect. Therefore, experiment E02-110 intends to measure the Q^2 dependence of the transparency T_A at fixed coherence length l_c .

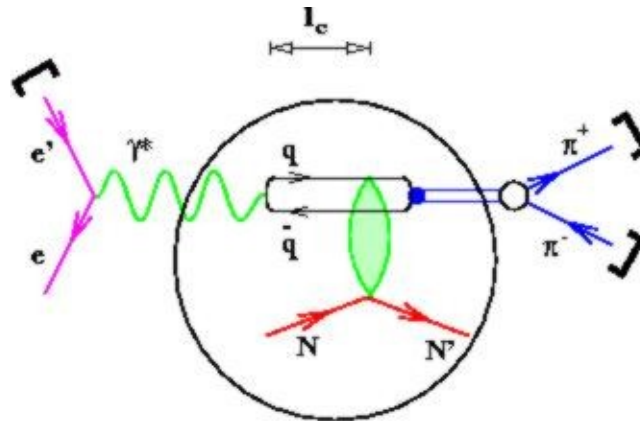


Fig. IV-3. Exclusive leptoproduction of the ρ^0 meson.

The experiment was performed using the CEBAF Large Acceptance Spectrometer (CLAS)⁷ in Hall B of the JLab. The data were taken with both 4 and 5 GeV electron beams incident on 4 cm liquid deuterium target and a solid target (0.4 mm thick ^{56}Fe and 1.72 mm thick ^{12}C) simultaneously. The run period was from December 2003 to March 2004. The data were recorded at an instantaneous luminosity of $2 \times 10^{34} \text{ cm}^{-2} \text{ s}^{-1}$. Figure IV-4 shows the projected uncertainties for complementary I_c

values to map the whole Q^2 region up to 4 GeV^2 using a 6 GeV electron beam and a 2 GeV photon beam on ^{56}Fe versus deuterium. Because the experiment was allocated only 70% of the approved beam time and the highest beam energy available was 5 GeV instead of 6 GeV, the photoproduction measurements will be performed later and the highest Q^2 the measurements will be 3 GeV^2 with a statistical error comparable to that proposed for 4 GeV^2 . The data analysis is in progress.

¹A. S. Carroll *et al.*, Phys. Rev. Lett. **61** 1698 (1988); Y. Mardor *et al.*, Phys. Rev. Lett. **81** 5085 (1998); A. Leksanov *et al.*, Phys. Rev. Lett. **87**, 212301 (2001).

²N. C. R. Makins *et al.*, Phys. Rev. Lett. **72**, 1986 (1994); T. G. O'Neill *et al.*, Phys. Lett. **B351**, 87 (1995); D. Abbott *et al.*, Phys. Rev. Lett. **80**, 5072 (1998); K. Garrow *et al.*, Phys. Rev. C **66**, 044613 (2002).

³E. M. Aitala *et al.*, Phys. Rev. Lett. **86**, 4773 (2001).

⁴A. Airapetian *et al.*, Phys. Rev. Lett. **90**, 052501 (2003).

⁵JLab experiment E02-110, " Q^2 Dependence of Nuclear Transparency for Incoherent ρ^0 Electroproduction", K. Hafidi, B. Mustapha, and M. Holtrop, spokespersons.

⁶B. Kopeliovich *et al.*, Phys. Rev. C **65**, 035201 (2002).

⁷B. Mecking *et al.*, Nucl. Instrum. Methods **A503/3**, 513 (2003).

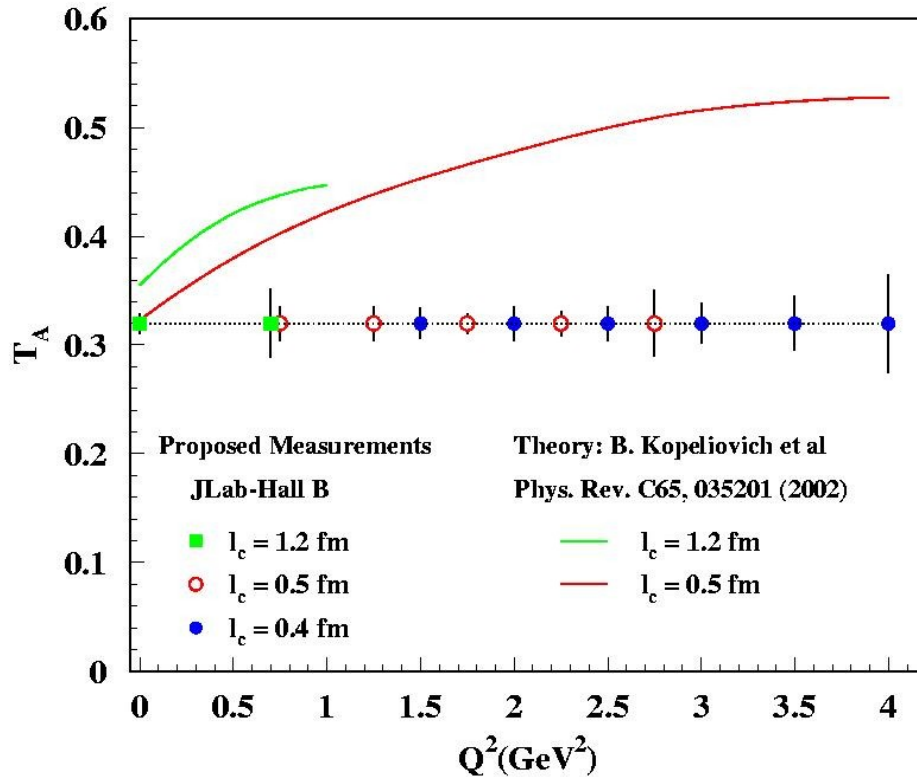


Fig. IV-4. Theoretical predictions and expected statistical accuracy.

b.2. Measurement of High Momentum Nucleons in Nuclei and Short Range Correlations

(J. Arrington, D. F. Geesaman, K. Hafidi, R. J. Holt, H. E. Jackson, P. E. Reimer, E. C. Schulte, X. Zheng, and the E02-019 Collaboration)

Inclusive scattering from nuclei at low energy transfer (corresponding to $x > 1$) is dominated by quasielastic scattering from nucleons in the nucleus. As the energy transfer decreases, the scattering probes nucleons of increasing momentum allowing us to map out the distribution of high momentum nucleons. These data can be used to constrain the high momentum components of nuclear spectral functions.¹ In addition, as the high momentum nucleons are dominantly generated by short-range correlations (SRCs), these data allow us to examine the strength of two-nucleon correlations in heavy nuclei.

Experiment E02-019² ran in late 2004 and measured inclusive scattering at large Q^2 over a broad range in x (up to $x = 3$). The high Q^2 values in this experiment should simplify the extraction of the high momentum components, as effects such as final state interactions are reduced at large Q^2 . The measurement focused on

^2H , ^3He , and ^4He , but data were also taken on several heavier nuclei. Measurements with few-body nuclei allow contact with theoretical calculations *via* essentially "exact" calculations for few-body systems. This can be used to study in detail contributions to the interaction beyond the impulse approximation (*e.g.*, final state interactions for scattering from correlated nucleons). Data on heavy nuclei can then be used to constrain the high momentum components of their spectral functions, as well as allowing an extrapolation to infinite nuclear matter.

These data provide sensitivity to the extremely high momentum components of the nuclear wave function, probing nucleons with momenta in excess of 1000 MeV/c. This will improve our ability to study the structure of nucleon correlations in nuclei. Direct comparisons of heavy nuclei to deuterium at large x will allow us to map out the strength of two-nucleon

correlations in both light and heavy nuclei. These data are expected to be significantly more sensitive to the presence of multi-nucleon correlations. Just as the ratio of heavy nuclei to deuterium at $x \gtrsim 1.5$ shows that the distribution in heavy nuclei is dominated by two-nucleon correlations, a similar ratio of heavy nuclei to ${}^3\text{He}$ at $x \gtrsim 2.5$ may provide the first experimental signature of three-nucleon correlations. Figure IV-5 shows the yield from ${}^3\text{He}$ at 18° .

In addition to probing nucleon distributions and short-range correlations, these data fill in a significant void in

our knowledge of the nuclear structure function. Little data exist for nuclei at large x , yet such data are important in the study of scaling and duality in nuclei,³ higher twist effects,^{4,5} and nuclear dependence of the structure function.⁶ In addition the $x > 1$ structure function must be included in studies of the energy-momentum sum rule and analysis of the QCD moments.⁵ While E02-019 emphasized the study of the high momentum nucleons in nuclei, it also provides the data necessary for a variety of studies.

¹J. Arrington *et al.*, Phys. Rev. Lett. **82**, 2056 (1999).

²JLab experiment E02-019, "Inclusive Scattering from Nuclei at $x > 1$ and High Q^2 with a 6 GeV Beam", J. Arrington, D. B. Day, A. F. Lung, and B. W. Filippone, spokespersons.

³J. Arrington *et al.*, Phys. Rev. C **64**, 014602 (2001); J. Arrington, R. Ent, C. E. Keppel, J. Mammei, and I. Niculescu, nucl-ex/0307012.

⁴I. Niculescu, C. Keppel, S. Liuti, and G. Niculescu, Phys. Rev. D **60**, 094001 (1999).

⁵J. Arrington, R. Ent, C. E. Keppel, and I. Niculescu, in preparation.

⁶K. Egiyan *et al.*, Phys. Rev. C **68**, 014313 (2003).

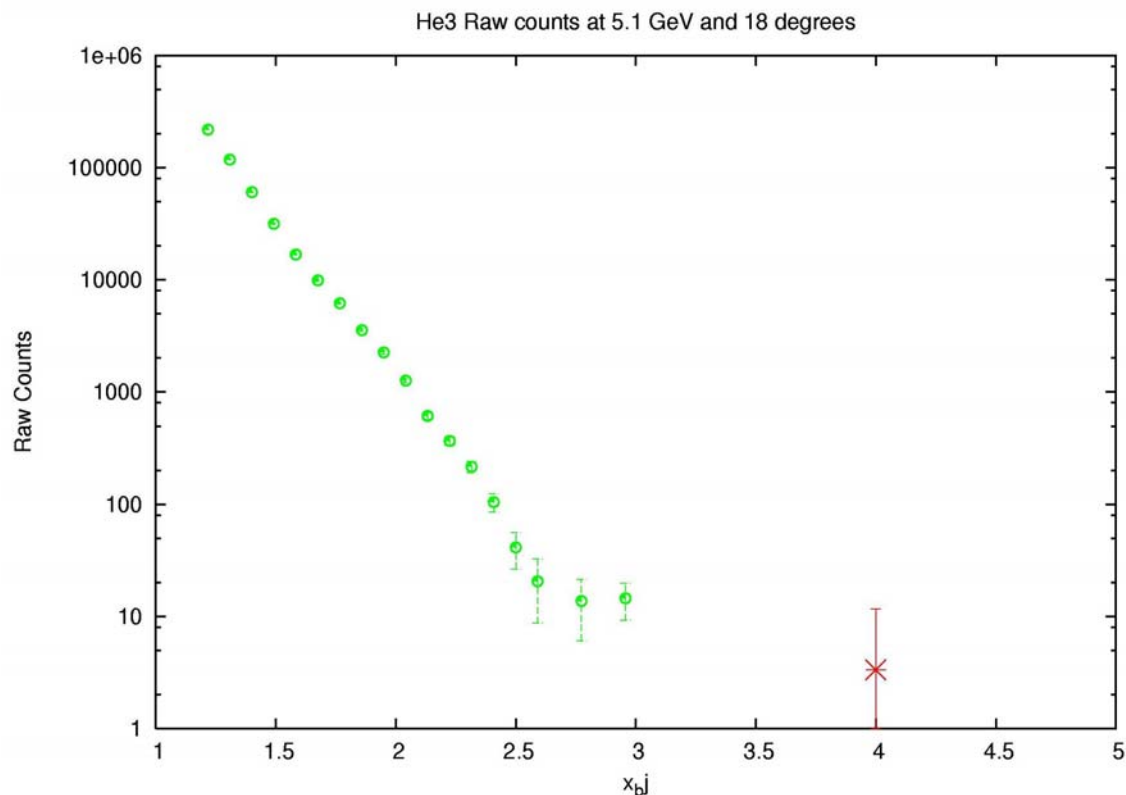


Fig. IV-5. Yield as a function of Bjorken x for the ${}^3\text{He}$ data at 18° . We have good statistics all the way up to $x = 3$, the kinematic endpoint for scattering from ${}^3\text{He}$. The red point shows the sum of counts above $x = 3$.

b.3. Measurement of the EMC Effect in Very Light Nuclei (J. Arrington, D. F. Geesaman, K. Hafidi, R. J. Holt, H. E. Jackson, D. H. Potterveld, P. E. Reimer, E. C. Schulte, X. Zheng, B. Zeidman, and the E03-103 Collaboration)

For more than twenty years, it has been known that the quark momentum distribution of nuclei is not simply the sum of the quark distributions of its constituent protons and neutrons. The structure function is suppressed in heavy nuclei at large values of x (corresponding to large quark momenta), and enhanced at low x values. Measurements to date indicate that the overall form of this modification is the same for all nuclei, but the magnitude of the enhancement and suppression is larger for heavier nuclei. Many attempts have been made to explain the EMC effect, but none of the proposed models can fully reproduce the observed modifications, and there is still no consensus on which effect or combination explain the data.

Experiment E03-103¹ ran in Hall C in late 2004 and measured the EMC effect for ³He, ⁴He, and a series of heavier nuclei. Because ⁴He has an anomalously large density for a light nucleus, it is the most sensitive test to determine if the EMC effect scales with A or with nuclear density. More importantly, these measurements of the EMC effect can be

compared to exact few body calculations. If the EMC effect is caused by few nucleon interactions, the universal shape observed in heavy nuclei may be a result of a saturation of the effect, and the shape may be different in few-body nuclei. While most existing data on heavy nuclei show the same x -dependence, there are hints of an A -dependence at large x values,² and calculations³ predict significantly different dependences for very light nuclei. By making precise measurements in light nuclei, we will be able to distinguish between different models of the EMC effect based on their predictions for few-body nuclei.

Finally, a measurement of $A \leq 4$ nuclei will help constrain models of the EMC effect in deuterium. Models of nuclear effects in deuterium and ³He must be used to extract information on neutron structure, and a high precision measurement including ¹H, ²H, ³He, and ⁴He will give a single set of data that can be used to evaluate these models in several light nuclei. This will help to quantify the model dependence of the neutron structure functions inferred from measurements on ²H and ³He.

¹JLab experiment E03-103, "A Precise Measurement of the Nuclear Dependence of the EMC Effect in Light Nuclei", J. Arrington and D. Gaskell, spokespersons.

²J. Arrington, R. Ent, C. E. Keppel, J. Mammei, and I. Niculescu, nucl-ex/0307012.

³G. I. Smirnov *et al.*, Eur. Phys. J. C **10**, 239 (1999); V. V. Burov *et al.*, Phys. Lett. **B466**, 1 (1999); I. R. Afnan *et al.*, Phys. Rev. C **68**, 035201 (2003); O. Benhar, V. Pandharipande, and I. Sick, Phys. Lett. **B410**, 79 (1997); O. Benhar, private communication.

b.4. Proton Polarization Angular Distribution in Deuteron Photo Disintegration (R. J. Holt, J. Arrington, K. Hafidi, P. E. Reimer, E. C. Schulte, K. Wijesooriya, and JLab E00-007 Collaboration)

The overall goal of experiment¹ E00-007 is to determine the mechanism that governs photoreactions in the GeV energy region. Our previous measurements² of induced polarization in deuteron photodisintegration produced surprising results at photon energies between 1 and 2 GeV. First these results disagreed markedly with previous experiments and secondly there was a remarkable disagreement with the meson-exchange model. The induced polarizations above 1 GeV and at $\theta_{\text{cm}} = 90^\circ$ were near zero, consistent with hadron helicity conservation. The goal of this experiment was to determine the

angular dependence of the polarization. Data were taken for a photon energy of 2 GeV and at five center-of-mass angles: 37° , 53° , 70° , 90° and 110° . The induced polarizations as well as polarization transfers were measured. A new polarimeter that contains both a C and a CH₂ scatterer was used for this experiment.

A significant problem arose in the analysis of the data because of the new "G0 delay by eight" helicity bit-reporting mode. Because the intended time markers in the data stream were not recorded with 100% efficiency, the helicity flags had to be reconstructed with great care. The

extracted form factor ratio agrees well with previous results.

¹JLab proposal E00-007, "Proton Polarization Angular Distribution in Deuteron Photodisintegration", R. Gilman, R. J. Holt, and Z.-E. Meziani, spokespersons.

²K. Wijesooriya *et al.*, Phys. Rev. Lett. **86**, 2975 (2001).

b.5. Measurements of the Nuclear Dependence of $R = \sigma_L/\sigma_T$ at Low Q^2 (J. Arrington, D. F. Geesaman, T. G. O'Neill, D. Potterveld, and the E99-118 Collaboration)

Inclusive electron scattering is a well-understood probe of the partonic structure of nucleons and nuclei. Deep inelastic scattering has been used to make precise measurements of nuclear structure functions over a wide range in x and Q^2 . The ratio $R = \sigma_L/\sigma_T$ has been measured reasonably well in deep inelastic scattering at moderate and high Q^2 using hydrogen and deuterium targets. However, R is still one of the most poorly understood quantities measured in deep inelastic scattering and few measurements exist at low Q^2 or for nuclear targets. Existing data rule out significant nuclear effects in R only at moderate to large values of Q^2 .

JLab experiment E99-119 is a direct measurement of R at low x and low Q^2 . The experiment was performed in July of 2000 and data were taken for hydrogen, deuterium, and heavier nuclei. The data are largely analyzed, but the cross section extraction at extremely small values of x and Q^2 involve large radiative corrections. While the radiative corrections will limit the region for which R can be extracted, these data are ideal for testing the radiative correction procedures in these extreme kinematics, and in particular the corrections coming from the nuclear elastic contributions. The final results for hydrogen and deuterium will be available soon and the analysis of the nuclear targets, with the larger radiative corrections, will be available shortly thereafter.

b.6. Electroproduction of Kaons and Light Hypernuclei (J. Arrington, K. Bailey, F. Dohrmann, D. F. Geesaman, K. Hafidi, B. Mueller, T. G. O'Neill, D. H. Potterveld, P. E. Reimer, B. Zeidman, and the E91-016 Collaboration)

JLab experiment E91-016 "*Electroproduction of Kaons and Light Hypernuclei*" is a study of the production of kaons on targets of H, D, ³He, and ⁴He at an incident electron energy of 3.245 GeV and $Q^2 \approx 0.37$ GeV². For H and D targets, additional data were obtained at an energy of 2.445 GeV and $Q^2 \approx 0.5$ GeV². The scattered electrons and emergent kaons were detected in coincidence with the use of the HMS and SOS spectrometers in Hall C. In addition to obtaining spectra, angular distributions were measured at forward angles with respect to the virtual photons.

The fundamental interaction being studied is the $N(e,e'K^+)Y$ where Y is either Λ or Σ and N is a nucleon, either free or bound in a nucleus. For H, the final state can only be a Λ or Σ^0 , with a missing mass spectrum consisting of two sharp peaks. For heavier targets, however, not only can Σ^- be produced on the neutron, but the relative motion of the bound nucleons results in quasi-free broadening of the peaks. Since there is no known bound state in the

mass 2 hyper-nuclear system, only quasi-free production is observed. For the heavier targets, ^{3,4}He, both Fermi broadening and a rapidly increasing number of final state configurations makes it more difficult to separate the various contributions. Because of the small mass difference between Σ^0 and Σ^- , distinguishing between these contributions is not possible without assuming that the Λ/Σ^0 ratio is the same as that for the free proton. Subtraction of the normalized Σ^0 contribution yields the first accurate value for Σ^- production on the neutron. In the above cases, the final state consists of the kaon, the hyperon, and the spectator nucleons from the target nucleus. For the ³He and ⁴He targets, one can also have final states consisting of only the kaon and a hypernucleus, where the produced hyperon is bound in the strangeness = 1 hypernucleus. Finally, the excellent particle identification and large phase space acceptance allowed an ancillary study of the electroproduction of ω mesons on the proton.

The kaon and ω electroproduction measurements from this experiment have formed the basis of five Ph.D.

theses. In 2004, the angular distributions of kaon electroproduction from ${}^3\text{He}$ and ${}^4\text{He}$ yielding bound hypernuclei¹ (Fig. IV-6) and measurements of ω electroproduction² were published. The results of the

measurements of Λ and Σ production from the proton as well as Λ , Σ and Σ^0 production from light nuclei are being prepared for publication.

¹F. Dohrmann *et al.*, Phys. Rev. Lett. **93**, 242501 (2004).

²P. Ambrozewicz *et al.*, Phys. Rev. C **70**, 035203 (2004).

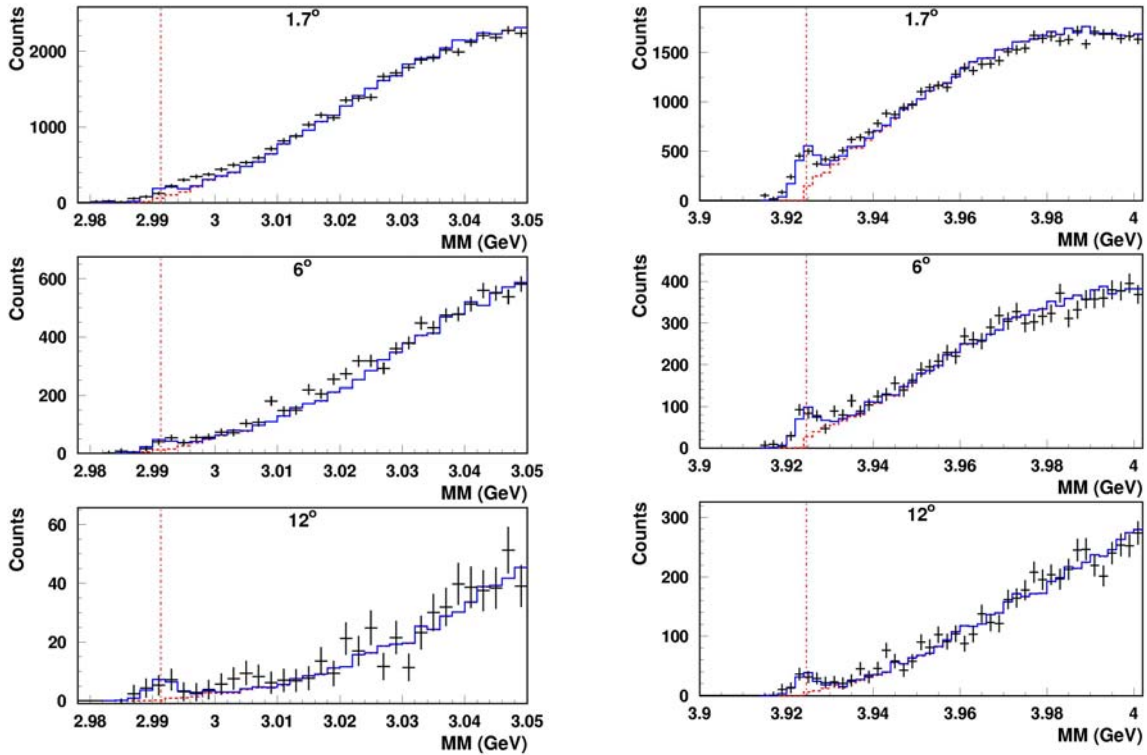


Fig. IV-6. Reconstructed missing mass spectra for ${}^3\text{He}$ (left) and ${}^4\text{He}$ (right) in the region of quasifree Λ production. The dashed lines are the simulations of the quasifree reactions ${}^{3,4}\text{He}(e,e'K^+)$, while the solid lines include the bound state reaction ${}^{3,4}\text{He}(e,e'K^+) {}_{\Lambda}^{3,4}\text{H}$. The thresholds for quasifree production are denoted by vertical lines.

C. QUARK STRUCTURE OF MATTER

c.1. The Structure of the Pion (P. E. Reimer, R. J. Holt, and K. Wijesooriya)

The light mesons have a central role in nucleon and in nuclear structure. The masses of the lightest hadrons, the mesons, are believed to arise from chiral symmetry breaking. The pion, being the lightest meson, is particularly interesting not only because of its importance in effective theories, but also because of its importance in explaining the quark sea in the nucleon and the nuclear force in nuclei. Most of our information about the pion structure in the valence region originates from pion-induced Drell-Yan reactions on a W target.¹ A long-standing mystery is the marked deviation of the high- x pion structure from perturbative QCD. At a Q^2 of 16 GeV² where Drell-Yan measurements are performed, one might expect perturbative QCD to be valid. In addition, the high- x behavior of the pion structure was questioned² recently on more fundamental grounds. We have re-analyzed the Drell-Yan data and made the following

improvements: Next-to-leading order analysis, modern nucleon parton distributions, modern nuclear effects in W and a less-restrictive parameterization of the pion structure function. While the results of this re-analysis indicate that the pion's valence parton distributions at high- x deviates significantly from the earlier leading-order analysis and is in better agreement with Dyson-Schwinger calculations as well as perturbative QCD, there remains substantial disagreement with these calculations.

Unfortunately, existing pion-nucleon Drell-Yan scattering data have limited x -resolution in the high- x region, and this may skew the interpretation of these data. Studies are being made to determine the feasibility of new measurements of the pion-nucleon Drell-Yan process using the E906 apparatus at Fermilab to determine if better x -resolution is achievable.

¹J. S. Conway *et al.*, Phys. Rev. D **39**, 92 (1989).

²M. B. Hecht *et al.*, Phys. Rev. C **63** 025213 (2001).

c.2. Studies of Nucleon Spin Structure and Related Measurements of Deep-Inelastic Scattering at HERA (H. E. Jackson, A. El Alaoui, K. G. Bailey, T. P. O'Connor, K. Hafidi, D. H. Potterveld, P. E. Reimer, Y. Sanjiev, and the HERMES Collaboration)

HERMES, HERA measurement of spin, is an international collaboration of 30 institutions formed to address a basic question of hadron structure. How do the spins of its constituent quarks combine with the spin of the glue and the angular momentum of the partons to give the proton its spin of 1/2? The HERMES experiment uses polarized internal targets in the HERA 30 GeV e^+/e^- storage ring at the DESY Laboratory. By emphasizing semi-inclusive deep-inelastic scattering (DIS) in which an identified hadron is observed in coincidence with the scattered lepton, HERMES has brought a new dimension to studies of nucleon spin structure. HERMES achieved a new milestone recently with the completion and publication¹ of a quark-flavor decomposition of the spin of the proton based on measurements of semi-inclusive double spin asymmetries which avoids the need for use of data from hyperon decay and the assumption of SU(3) symmetry. This is the first such measurement using target double-spin asymmetries

for charged pions and kaons. In contrast to previous results based solely on inclusive measurements, all extracted sea quark polarizations are consistent with zero, and within experimental errors the light quark sea helicity densities are flavor symmetric. The measurement was one of the principal objectives of the HERMES program as originally conceived.

Current activities, which are scheduled to continue through October of 2005, are focused on measurements with a transversely polarized target which probes the effects of transverse motion of the quarks. The single-spin asymmetries under study are related to the third structure function, transversity, required to describe nucleon spin structure in leading order. Results of the first phase of this study which have just appeared² have been used for the first time to extract the signal for the quark transversity as generated by the Collins fragmentation process. From the same data a signal has been extracted for a correlation between transverse target

polarization and intrinsic transverse momentum of quarks as represented by the previously unmeasured Sivers distribution function. In an analysis to be reported shortly, these data have been combined with previously reported results for longitudinally polarized proton targets to evaluate the subleading-twist contributions to the longitudinal case.

In 2006 the focus of the HERMES program will change with the installation of a large acceptance recoil detector which will enhance the solid angle acceptance and missing mass resolution in measurements of hard exclusive processes such as electroproduction of mesons and real photons (deeply virtual Compton scattering). HERMES already has studied several exclusive reactions, including exclusive production of charged and neutral pions, and of ρ mesons. Recent measurements of deeply virtual Compton scattering include the first measurements of a beam-charge asymmetry. The intense interest in these processes stems from their description in terms of Generalized Parton Distributions (GPDs) which are expected to provide access to the quark total angular momentum content of the nucleon. With the new detector, the exclusivity of events will be established by positive identification of the recoil proton and measurement of its recoil momentum. The enhanced selectivity of

these measurements will provide a unique opportunity to assess the promise of GPDs as the next step in understanding the spin structure of the nucleon.

A very productive program of measurements of unpolarized DIS continues with the use of high-luminosity dedicated running exclusively for HERMES during the last hour of each fill of the HERA e^+/e^- storage ring. Attempts to isolate and confirm a previously reported signal for the existence of a 5-quark exotic baryon state at 1540 MeV³ continue with the installation of an event trigger designed to select events with the expected pentaquark decay topology. Studies of quark propagation in nuclear matter are continuing with measurements of the ratio of hadron multiplicities in heavy targets to those in deuterium. Data on the kinematic dependences of these ratios as measured for different hadron types provide new insights into the propagation process. Data on the multiplicities measured for proton and deuteron targets currently under analysis will shortly provide accurate measurements of quark fragmentation functions specifically at HERMES kinematics, and provide a rigorous test of factorization. The HERA accelerator will continue operations through the summer of 2007. Every effort is being made to maximize the impact of the beam time that remains. Highlights of recent results are presented below.

¹A. Airapetian *et al.*, Phys. Rev. D **71**, 012003 (2005).

²A. Airapetian *et al.*, Phys. Rev. Lett. **94**, 012002 (2005).

³A. Airapetian *et al.*, Phys. Lett. **B585**, 213 (2004).

c.2.1. Polarization of the Strange Quark Sea in the Proton from Semi-Inclusive Deep-Inelastic Scattering on the Deuteron (H. E. Jackson, A. El Alaoui, K. G. Bailey, T. P. O'Connor, K. Hafidi, D. H. Potterveld, P. E. Reimer, Y. Sanjiev, and the HERMES Collaboration)

The polarization of the strange quarks in the proton is of particular interest, because an explanation of the small net contribution to the nucleon spin from the quark spins under the assumption of SU(3) symmetry implies a significant negative value for this quantity. Such a value would explain the violation of the Ellis-Jaffe sum rule in inclusive deep-inelastic scattering (DIS). However, recent results from HERMES for a flavor decomposition of quark helicity distributions based on semi-inclusive DIS suggest that the polarization of the strange sea is zero or slightly positive. The data are shown in Fig. IV-7. The total strange quark helicity density $\Delta S(x) \equiv \Delta s(x) + \Delta \bar{s}(x)$ carries no isospin. It can be extracted from

measurements of scattering from deuterium alone, which is isoscalar. Effectively, measurements of the inclusive spin asymmetries provide an estimate of the helicity density of the non-strange sea. Using the spin asymmetries measured for charged kaons as the second experimental data set, it is possible to extract directly $\Delta S(x)$. Furthermore, by measuring directly the charged kaon multiplicities at HERMES kinematics, the fragmentation functions relevant to the extraction procedure can be obtained without resort to other experiments. A direct leading-order extraction of $\Delta S(x)$ using this approach is in progress. Because, in contrast to the published data, only the more recently acquired deuterium database is used, the analysis can be carried out

with less stringent data restrictions and attendant higher statistics than that used in the analysis of Fig. IV-7. In parallel, with this effort, a similar analysis chain is being pursued with neutral kaons. With the combined treatment of the spin-asymmetries for

charged and neutral kaons a more accurate measure of $\Delta S(x)$ will be possible. The only assumption made in this analysis is charge-conjugation invariance, and no Monte-Carlo simulations of the fragmentation process are required.

¹A. Airapetian *et al.*, Phys. Rev. D **71**, 012003 (2005).

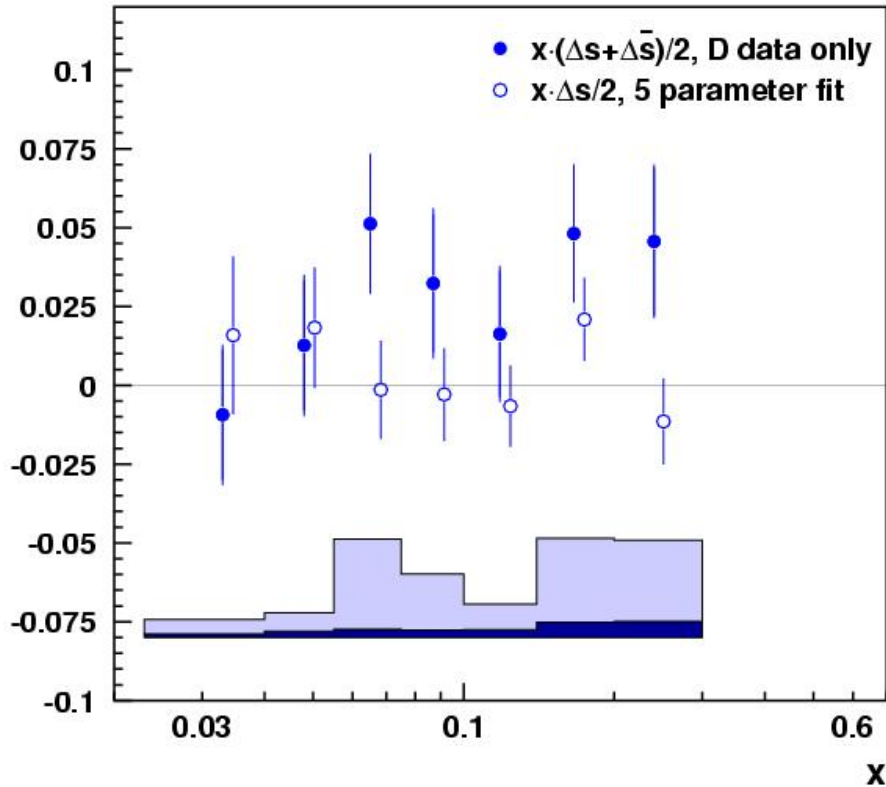


Fig. IV-7. The average strange quark helicity density $x \cdot [\Delta s(x) + \Delta \bar{s}(x)]/2$ from the isoscalar extraction method (full points). For comparison the open symbols denote the results from a five parameter fit, which are offset horizontally for presentation. Both data sets are taken from Ref. 1. The band in the bottom part gives the total systematic uncertainty on the results from the isoscalar extraction. The dark shaded area corresponds to the uncertainty from the input asymmetries, and the open part relates to the uncertainty in fragmentation functions.

c.2.2. Azimuthal Asymmetries and Transversity (H. E. Jackson, A. El Alaoui, K. G. Bailey, T. P. O'Connor, K. Hafidi, D. H. Potterveld, P. Reimer, Y. Sanjiev, and the HERMES Collaboration)

Single-spin asymmetries in the distribution of lepto-produced hadrons in the azimuthal angle around the virtual photon direction are a valuable tool for the exploration of transverse spin and momentum degrees of freedom in nucleon structure. Such asymmetries have been observed in semi-inclusive DIS with unpolarized beams and with targets polarized both longitudinally and transversely with

respect to the incident beam direction. Asymmetries have also been observed with polarized beams and unpolarized nucleons. The asymmetry for a transversely polarized target can be interpreted in terms of the Sivers and the transversity distribution functions, convoluted with the ordinary unpolarized and Collins fragmentation functions, respectively. HERMES recently published the first decomposition of these effects¹ using a transversely

polarized proton target. In the case of targets that are longitudinally polarized, the interpretation is more complex. The HERMES measured lepton asymmetries on a transverse target cited above have been used to eliminate the contribution due to the transverse spin component as seen by the virtual photon, from the measured asymmetries on a longitudinal polarized target, thereby allowing for the

first time, the extraction of the purely subleading twist contribution to the measured lepton asymmetries. This contribution is significantly positive for π^+ mesons and dominates the asymmetries on a longitudinally polarized target previously measured by HERMES. The subleading-twist contribution for π^- mesons is found to be small.

¹A. Airapetian *et al.*, Phys. Rev. Lett. **94**, 012002 (2005).

c.2.3. New Results for Collins and Sivers Asymmetries with a Transversely Polarized Target (H. E. Jackson, A. El Alaoui, K. G. Bailey, T. P. O'Connor, K. Hafidi, D. H. Potterveld, P. E. Reimer, Y. Sanjiev, and the HERMES Collaboration)

The first global evidence for both Collins and Sivers asymmetries was published by the HERMES collaboration in 2005.¹ These results were based on data recorded during the 2002-2003 running period. Running with a transversely polarized target has continued and nearly five times the statistics as was used in the first publication have been accumulated. Results for the unweighted Collins and Sivers moments have been extracted from the data using the same analysis procedures as in the earlier treatment. The Collins moment is generated by a $\sin(\Phi + \Phi_s)$

dependence on the angle Φ between the lepton scattering plane and the hadron production plane and on the target angle Φ_s between the target polarization and the lepton scattering plane. The corresponding dependence for the Sivers moment is $\sin(\Phi - \Phi_s)$. Non-zero values for these azimuthal moments are signatures for significant contributions from the Collins and Sivers effects. The new data shown in Figs. IV-8 and IV-9 confirm with much improved precision the trends observed in earlier measurements. Of particular note is the unexpectedly large Collins moment for negative pions.

¹A. Airapetian *et al.*, Phys. Rev. Lett. **94**, 012002 (2005).

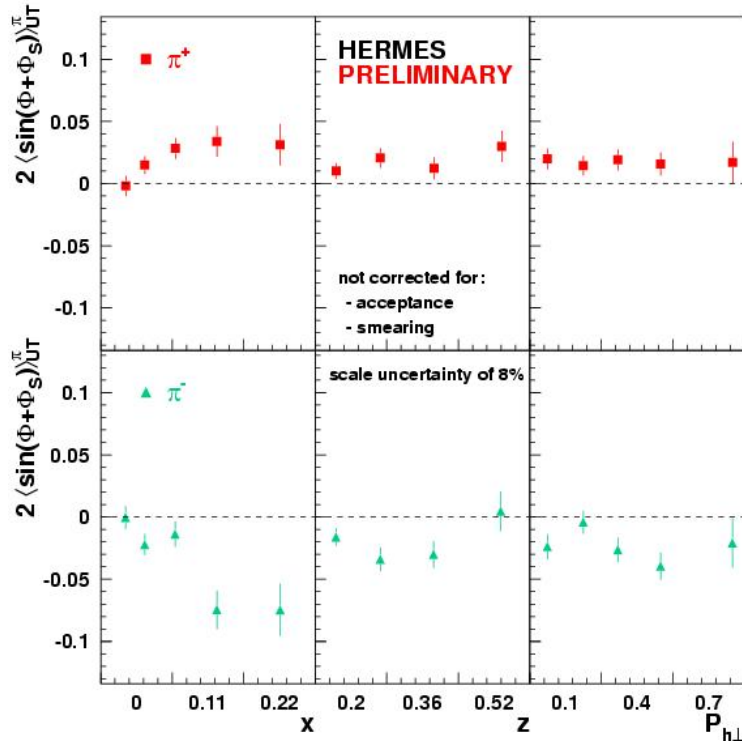


Fig. IV-8. Measured Collins moments for charged pions as a function of x , z , and $P_{h\perp}$. The error bars represent the statistical uncertainties.

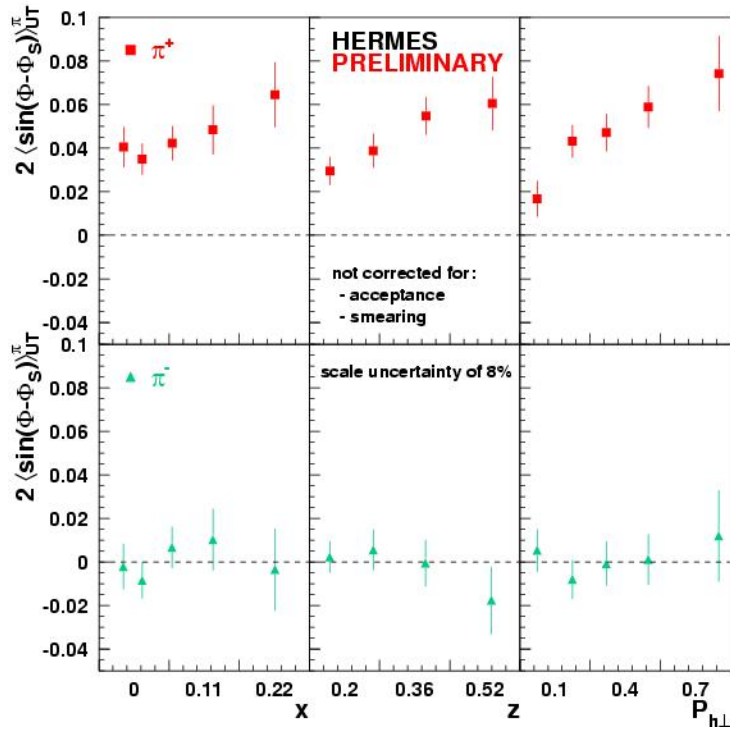


Fig. IV-9. Measured Sivers moments for charged pions as a function of x , z , and $P_{h\perp}$. The error bars represent the statistical uncertainties.

c.2.4. The Deuteron Tensor Polarized Structure Function b_1 (H. E. Jackson, A. El Alaoui, K. G. Bailey, T. P. O'Connor, K. Hafidi, D. H. Potterveld, P. E. Reimer, Y. Sanjiev, and the HERMES Collaboration)

The deep-inelastic scattering (DIS) of leptons by nucleons is characterized by four fundamental structure functions, F_1 , F_2 , g_1 , and g_2 . Polarized beams are required to measure the latter two, and the study of g_1 has been the primary focus of many experiments over the years. When a deuteron is the scatterer, there are four additional fundamental structure functions,¹ b_{1-4} , that arise because the deuteron has spin 1. They have not been measured to date. The first, b_1 , is of considerable interest. It is sensitive to differences in the quark momentum distributions between the 0 helicity (q_0) and the spin-averaged ± 1 helicity ($q^+ + q^-$) states of the hadron. Of leading twist, b_1 should be identically zero for a simple composition of nucleons in an s state. However, a non-zero value is possible through nuclear effects such as binding, the d state of the deuteron, and shadowing effects such as coherent double scattering.^{2,3} If non-zero, it should be taken

into account when extracting the neutron structure functions from deuterium data (hitherto it has been ignored). Moreover, a non-zero value could indicate that the quark sea becomes tensor polarized in the deuteron, which is unexpected in the naive quark model. The HERMES experiment has investigated the tensor spin structure of the deuteron using the 27.6 GeV positron beam of HERA. The use of a tensor polarized deuteron gas target with only a 0.01 residual vector polarization enabled the first measurement of the tensor asymmetry A_{zz}^d and the tensor structure function b_1^d in the kinematic range of the Bjorken variable $0.002 < x < 0.85$ and the squared four-momentum transfer $0.1 < Q^2 < 20 \text{ GeV}^2$. The results are presented in Fig. IV-10. The rise of b_1^d for decreasing values of x can be interpreted either as a significant tensor polarization of the quark sea in the deuteron, or as a shadowing effect in the context of coherent double-scattering models.

¹H. P. Hoodbhoy *et al.*, Nucl. Phys. **B312**, 571(1989).

²J. Edelmann *et al.*, Phys. Rev C **57**, 3392 (1998).

³K. Bora and R. L. Jaffe, Phys. Rev. D **57**, 6906 (1998).

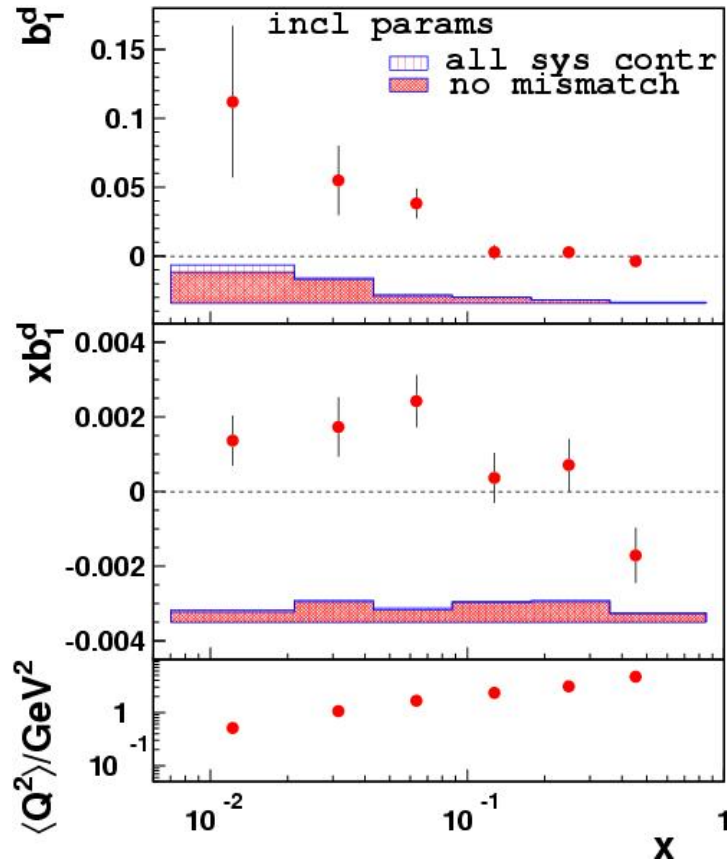


Fig. IV-10. The tensor structure function b_1^d . The error bars are statistical and the shaded bands show the systematic uncertainty, with and without the contribution from possible instrumental asymmetries. The middle panel shows the $x b_1^d$ distribution and the bottom panel shows the average value of Q^2 in each x -bin.

c.2.5. Measurements of Deeply-Virtual Compton Scattering at HERMES (H. E. Jackson, A. El Alaoui, K. G. Bailey, T. P. O'Connor, K. Hafidi, D. H. Potterveld, P. Reimer, Y. Sanjiev, and the HERMES Collaboration)

The concept of Generalized Parton Distributions (GPDs) has recently emerged and generated great interest as a means of studying the dynamics of quarks and gluons in a very general framework. The cleanest way to access GPDs is Deeply Virtual Compton Scattering (DVCS), the production of a real photon in hard exclusive electron scattering. In HERMES experiments the signature for DVCS is an azimuthal asymmetry in the angle ϕ , the azimuthal angle around the virtual photon direction between the lepton scattering plane and the production plane. It is attributed to the interference of the Bethe-Heitler and

DVCS processes. HERMES has already reported substantial beam-spin, target-spin, and beam-charge asymmetries in scattering from proton and deuteron targets. For the first time, DVCS has been measured for nuclear targets. DVCS off nuclei probes GPDs of nuclei, *i.e.*, measures quark properties in nuclei. At small $|t|$, where t is the usual Mandelstam variable, the interference term for heavy nuclei grows with the nuclear charge Z due to the growing Bethe-Heitler amplitude for coherent scattering. A comparison of the asymmetries for deuterium and neon targets is presented in Fig. IV-11. A significantly larger $\sin(\phi)$ moment is observed for neon.

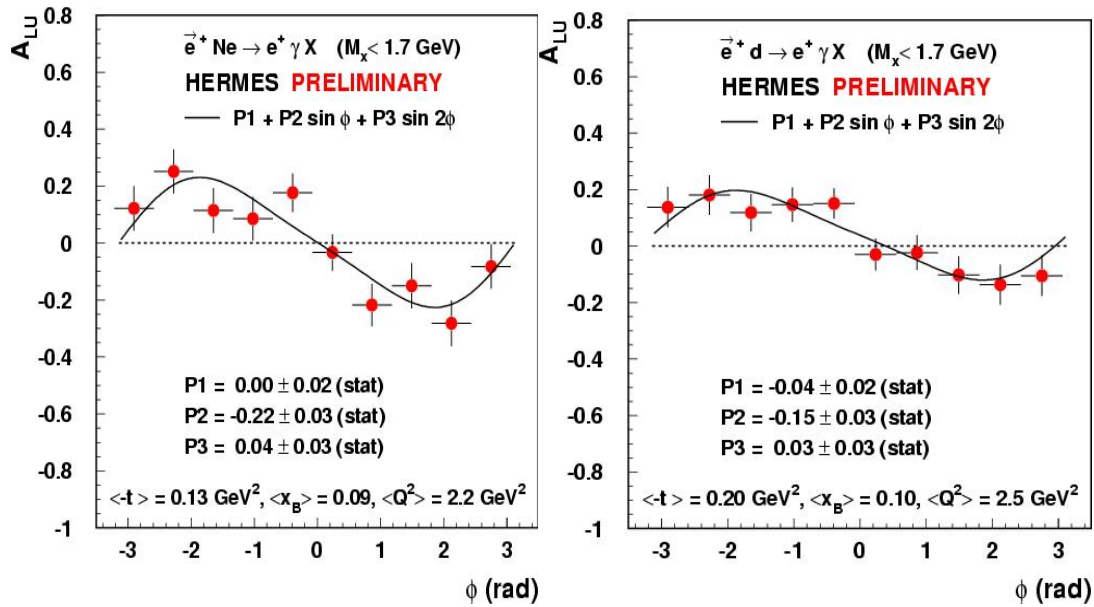


Fig. IV-11. Azimuthal beam charge asymmetries measured for deuterium and neon targets. The $\sin(\phi)$ contribution of the asymmetry for neon (left) is significantly larger than for a deuterium target (right).

c.2.6. Quark Fragmentation to Pions, Kaons, and Nucleons in the Nuclear Environment

(H. E. Jackson, A. El Alaoui, K. G. Bailey, T. P. O'Connor, K. Hafidi, D. H. Potterveld, P. E. Reimer, Y. Sanjiev, and the HERMES Collaboration)

HERMES continues to study the hadronization of quarks into identified hadron types by measuring the nuclear dependence of pion, kaon, and proton multiplicities in targets of krypton, neon, nitrogen, and helium relative to that of a deuterium target. The kinematic and mass dependences of the ratio of multiplicities for heavier targets to deuterium can provide useful constraints on models for the hadronization process. Recently, HERMES published the first data of this type for various identified hadrons, both charged and neutral. The data indicate different formation times for nucleons compared to those of pions and kaons. The data are consistent with an $A^{2/3}$ -dependence predicted by theoretical models which also predict an L^2

dependence on the energy loss of quarks traversing a path length L . HERMES continues to take data in an effort to test this prediction. As part of that effort, measurements have been made of multiplicity ratios for π^0 as a function of the virtual photon energy ν and the relative hadron energy z , and for charged pions, kaons, and (anti)protons as a function of transverse momentum. The 27 GeV data on ${}^4\text{He}$, ${}^{20}\text{Ne}$, and ${}^{84}\text{Kr}$ nuclear targets have been used and the results measured in terms of the ratio of the number of hadrons produced per DIS event for a nuclear target to that on a deuterium target. Figure IV-12 shows the dependence of this ratio on the transverse momentum. The results obtained are sensitive to the production length in the hadronization process on nuclei.

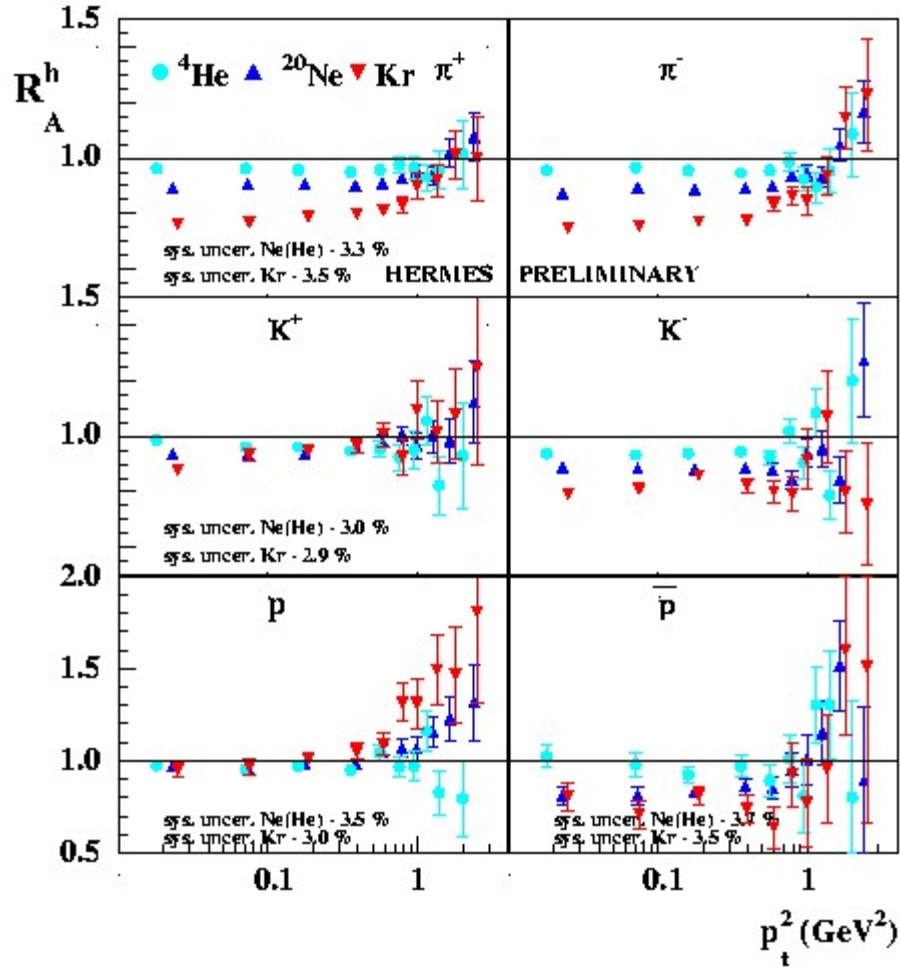


Fig. IV-12. R^h as a function of p_t^2 for π^\pm , K^\pm , and (anti)protons for different nuclei.

c.2.7. Extraction of Hadron Multiplicities from Deep-Inelastic Scattering Data

(H. E. Jackson, A. El Alaoui, K. G. Bailey, T. P. O'Connor, K. Hafidi, D. H. Potterveld, P. E. Reimer, Y. Sanjiev, and the HERMES Collaboration)

The semi-inclusive production of pseudoscalar mesons in deep-inelastic scattering (DIS) provides an excellent test of the accuracy of the quark-parton

model and QCD as a description of DIS at HERMES kinematics. In the QCD improved quark-parton model, the hadron multiplicities are given by the expression

$$\frac{1}{N_{DIS}(Q^2)} \frac{dN^h(z, Q^2)}{dz} = \frac{\sum_f e_f^2 \int_0^1 dx q_f(x, Q^2) D_f^h(z, q^2)}{\sum_f e_f^2 \int_0^1 dx q_f(x, Q^2)}$$

The fragmentation function D_f^h is a measure of the probability that a quark of flavor f fragments into a hadron h of energy E_h . The dependence of the multiplicities on x , z and Q^2 provide direct tests of scaling as well as measures of isospin invariance. They also provide an excellent constraint on Monte

Carlo simulations of the DIS process. HERMES is carrying out a careful determination of the multiplicities for charged hadrons individually identified as pions, kaons, or nucleons using the HERMES RICH particle identification system. The final multiplicities for both charges of pions and kaons are presented in Fig. IV-13.

These data resulted from a special mode of end of fill running at the HERA accelerator in which unpolarized targets of high density provide strongly

enhanced specific luminosities compared to normal polarized operation.

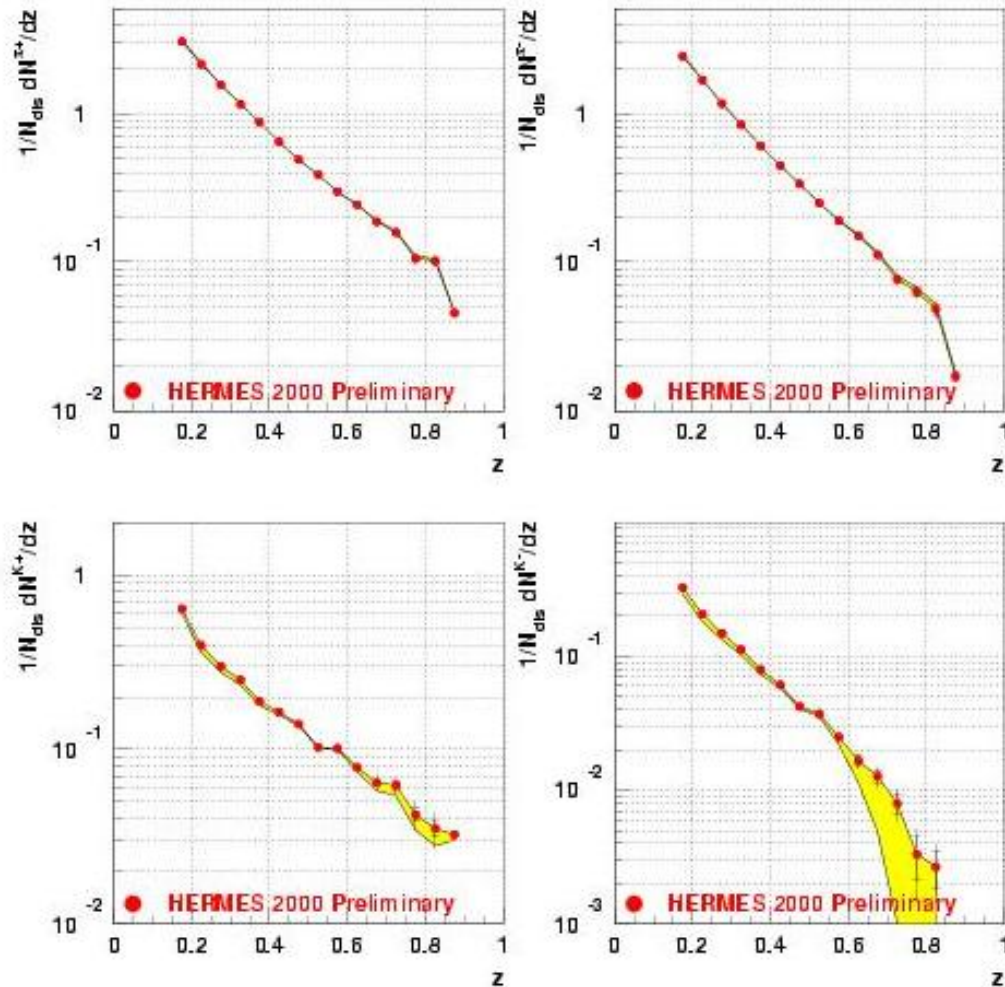


Fig. IV-13. The multiplicities versus z , including all corrections and evolved to $Q_0^2 = 2.5 \text{ GeV}^2$. The yellow band depicts the systematic error due to RICH PID unfolding.

c.2.8. Search for an Exotic $S = -2, Q = -2$ Baryon Resonance with Mass Near 1862 MeV
 (H. E. Jackson, A. El Alaoui, K. G. Bailey, T. P. O'Connor, K. Hafidi, D. H. Potterveld, P. E. Reimer, Y. Sanjiev, and the HERMES Collaboration)

The prediction of narrow exotic baryon resonances based on the chiral solution model has triggered an intensive search for the exotic members of an antidecuplet with spin 1/2. In this antidecuplet, all three vertices are manifestly exotic. The lightest exotic member lying at its apex, named the Θ^+ , is predicted to have a mass near 1530 MeV and a

narrow width. Its existence is currently the subject of considerable controversy. Experimental evidence for a second exotic member of the antidecuplet came from the reported observation of a $S = -2, Q = -2$ baryon resonance in proton-proton collisions at $\sqrt{s} = 17.2 \text{ GeV}$ at the CERN SPS.¹ HERMES has searched for an exotic baryon resonance with $S = -2, Q = -2$ in quasireal

photoproduction on a deuterium target by looking for the decay through the channel $\Xi^- \pi^- \rightarrow p \pi^- \pi^- \pi^-$. No evidence for a previously reported $\Xi^-(1860)$ resonance is found in the $\Xi^- \pi^-$ invariant mass

spectrum. An upper limit for the photoproduction cross section of 2.1 nb is found at the 90% confidence level. The photoproduction cross section for the $\Xi^0(1530)$ is found to be between 9 and 24 nb.

¹C. Alt *et al.* (NA49 Collaboration), Phys. Rev. Lett. **91**, 232003 (2003).

c.2.9. Study of Factorization and Flavor Content of the Nucleon in Unpolarized Semi Inclusive Deep Inelastic Scattering at HERMES (K. Hafidi, A. El Alaoui, K. G. Bailey, T. P. O'Connor, H. E. Jackson, D. Potterveld, P. E. Reimer, and the HERMES Collaboration)

Semi Inclusive Deep Inelastic Scattering (SIDIS) has been used extensively in recent years as an important testing ground for QCD. Indeed, SIDIS offers a great opportunity for studying the spin and the flavor content of the nucleon. However, using SIDIS relies on the factorization assumption between the hard scattering process and the hadronization of the struck quark. Although at high energy the scattering and production mechanisms factorize, it remains unclear to what extent factorization applies at lower energies. HERMES has shown that within the experimental precision which was dominated by the statistical error, factorization works reasonably well at the HERMES kinematics conditions.¹ By accumulating an order of magnitude more statistics, it is now

possible to perform a more precise test of factorization.

In this analysis, all HERMES unpolarized and averaged polarized hydrogen and deuterium data have been used. Four independent yields have been determined; $Y_p^{\pi^+}(x,z)$, $Y_p^{\pi^-}(x,z)$, $Y_n^{\pi^+}(x,z)$ and $Y_n^{\pi^-}(x,z)$ for fixed x -bins as a function of z , where z is the fraction of photon energy carried by the detected hadron. The neutron yield can be obtained from the deuteron yield via $Y_d^{\pi^-} = (Y_p^{\pi^-} + Y_n^{\pi^-})/2$. Assuming isospin symmetry between protons and neutrons $u_p(x) = d_n(x)$, $d_p(x) = u_n(x)$ as well as charge conjugation invariance $\bar{u}_p(x) = \bar{d}_n(x)$, $\bar{d}_p(x) = \bar{u}_n(x)$, one can form two ratios in which the fragmentation functions cancel out:

$$R_1(x) = \frac{Y_p^{\pi^+} + Y_p^{\pi^-}}{Y_d^{\pi^+} + Y_d^{\pi^-}} = \frac{2}{5} \frac{4u(x) + d(x) + 4\bar{u}(x) + \bar{d}(x)}{u(x) + d(x) + \bar{u}(x) + \bar{d}(x)}$$

$$R_2(x) = \frac{Y_p^{\pi^+} - Y_p^{\pi^-}}{Y_d^{\pi^+} - Y_d^{\pi^-}} = \frac{1}{3} \frac{4u(x) - d(x) - 4\bar{u}(x) + \bar{d}(x)}{u(x) + d(x) - \bar{u}(x) - \bar{d}(x)}$$

Defining the valence quark distribution as: $q_v(x) = q(x) - \bar{q}(x)$ the sea contribution cancels exactly in the difference of charge multiplicities and

one obtains the following expression for the valence $d_v(x)/u_v(x)$ ratio:

$$\frac{d_v(x)}{u_v(x)} = \frac{4 - 3R_2(x)}{1 + 3R_2(x)}$$

The observation of the z -scaling behavior of $R_1(x)$ and $R_2(x)$ would be a test of factorization. In such case, the yield ratios R_1 and R_2 will be a direct measurement of the quark distributions and not related to the fragmentation functions. The kinematic range is $0.02 < x < 0.6$ at the average Q^2 of 2.5 GeV^2 . The expected statistical precision of the ongoing analysis represents a considerable

improvement of our ability to check factorization. In addition, measuring d_v/u_v will provide an additional test of factorization by comparing HERMES result with QCD fit of other high energy data.

In conclusion, with the ongoing analysis, we will be able to quantify with high precision the validity of the factorization assumption. We will also extract the

valence quark distribution ratio of the nucleon d_v/u_v using π^+/π^- yield ratios on hydrogen and deuterium.

¹K. Ackerstaff *et al.*, Phys. Rev. Lett. **81**, 5519 (1998).

²EMC Collaboration and J. Ashman *et al.*, Z. Phys. C **52**, 361 (1991).

³G. T. Jones *et al.*, Z. Phys. C **62**, 601 (1994).

c.3. Measurement of the Absolute Drell-Yan Cross Section on Hydrogen and Deuterium
(P. E. Reimer, D. F. Geesaman, S. B. Kaufman, N. C. R. Makins, B. A. Mueller and the FNAL E866/NuSea Collaboration)

Very little is known about the regime in which only one parton carries much of proton's momentum – different theoretical treatments prescribe different behaviors as $x \rightarrow 1$ (where x represents the fraction of the proton's momentum carried by the interacting parton) and there is very little data available to serve as a guide. In the fixed target environment, the Drell-Yan process is sensitive to the high- x behavior of the *beam's* quarks and the low- and intermediate- x behavior of the target antiquarks. E866 has measured the absolute cross sections for *proton-proton* and *proton-deuterium* Drell-Yan.¹ As $x \rightarrow 1$, these data

are dominated by the beam proton's quark distribution of $4u(x)+d(x)$. The measured absolute cross sections, relative to a next-to-leading order (NLO) calculation are shown in Fig. V-14. Recent work has focused on calculating the effect of radiative corrections to the Drell-Yan cross section. These corrections appear to account for approximately 3-5% of the effect at large- x , and intermediate- x . As can be seen in Fig. V-14, the quark distributions used in the calculation *over predict* the measured cross sections at large- x by a significant amount.

¹J. C. Webb *et al.* (Fermilab E866/NuSea Collaboration), "Absolute Drell-Yan Dimuon Cross Sections in 800 GeV/c pp and pd Collisions", submitted to Phys. Rev. Lett., hep-ex/0302019.

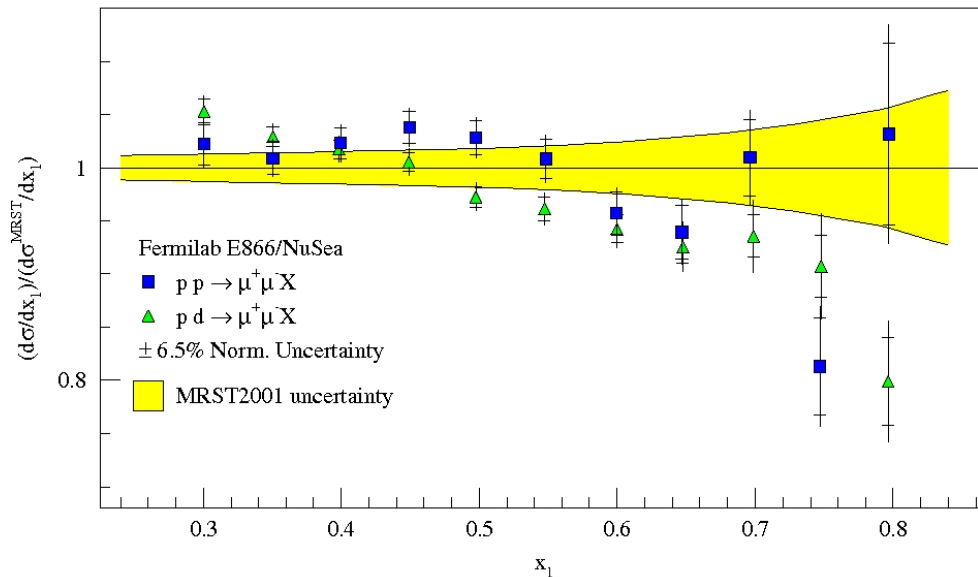


Fig. V-14. The ratio of Drell-Yan cross section (including radiative corrections) measured by Fermilab E866/NuSea for proton-deuterium (triangles) and proton-proton (squares) to calculated NLO cross section based on the MRST2001 parton distributions. The yellow band represents the uncertainty given by MRST2001 on $4u(x) + d(x)$.

c.4. Drell-Yan Measurements with 120 GeV Protons, FNAL E906 (P. E. Reimer, D. F. Geesaman, J. Arrington, K. Hafidi, R. J. Holt, D. H. Potterveld and the FNAL E906 Collaboration)

The proton and the neutron are composite objects, made of quarks, antiquarks and gluons, collectively known as partons. While many of the properties of the proton may be attributed to its three valence quarks, it is, in fact, much more complicated, with over 50% of its momentum being carried by the its non-valence (sea) quarks and gluons. To understand the structure of the proton, it is necessary to understand the sea quarks, their origins and their interactions with the gluons that bind the proton together. E906 is specifically designed to use Drell-Yan scattering to probe the sea quarks of the proton.¹

The Drell-Yan mechanism provides a powerful tool to study the structure of the proton at the quark level. In Drell-Yan scattering a quark (or antiquark) in the proton beam annihilates with an antiquark (or quark) in the target. The resulting annihilation produces a virtual photon that decays into a pair of leptons, which are seen in the detector. The kinematics of the detected leptons can be used to select interactions between beam valence quarks and target antiquarks. This was successfully exploited by Fermilab E866/NuSea using an 800 GeV/c proton beam provided new insight into the antiquark sea in the proton^{2,3} and nuclear dependence phenomena.⁴ FNAL E906 has been approved by Fermilab to extend Drell-Yan measurements to larger values of x (the fraction of the proton's momenta carried by the struck quark) using the new 120 GeV Main Injector at Fermilab. The new data obtained by this experiment will address several outstanding questions.

Vacuum polarization accounts for the creation of a flavor symmetric sea. Previous E866 Drell-Yan data, however, exhibit a large asymmetry between \bar{d} and \bar{u} for $x < 0.25$ (where x represents the fraction of the protons momentum carried by the interacting quark) clearly indicating a non-perturbative origin to the sea. Above $x > 0.28$ these data, albeit with poor statistical uncertainty, indicate the ratio \bar{d}/\bar{u} returns to unity. This result dramatically changed the sea quark parton distribution fits and was completely unpredicted by meson cloud and other non-perturbative models. The return of \bar{d}/\bar{u} to unity clearly signals a change in the mechanism by which the sea is generated.^{2,3,5} Fermilab E906 will determine \bar{d}/\bar{u} and $\bar{d} - \bar{u}$ for $0.1 \leq x \leq 0.45$, encompassing the non-perturbative region and extending well into the region where the sea appears to

return to symmetry, allowing for the study of the relative importance of the perturbative and non-perturbative sea. The current parton distributions now reproduce the previous Drell-Yan data for $0.28 < x < 0.3$, but allow $\bar{d}/\bar{u} < 1$ as x increases above 0.3. This is not expected by *any* models of the proton, either meson or perturbative, and is simply indicative of the complete lack of data. E906 will provide this data, as shown in Fig. V-15.

Very little is known about the regime in which only one parton carries much of proton's momentum – different theoretical treatments prescribe different behaviors as $x \rightarrow 1$ and very little data is available to serve as a guide. Through the partons in the beam proton, Fermilab E906 will access these distributions. The Drell-Yan cross section is dominated by the distribution of $4u(x) + d(x)$ as $x \rightarrow 1$. E906 will extend the data provided by Fermilab E866 to higher x and provide much more precise *proton* data than is currently available.

Models based on the hypothesis that nuclear binding is governed by the exchange of mesons have been used to quite successfully describe the nuclear force. Given the success of these models, it is natural to look for direct experimental evidence for the presence of these mesons in nuclei. Thus far, however, no direct evidence has been found.⁶ If present, these mesons will lead to an enhancement of antiquarks in the nucleus, and Drell-Yan is ideally suited to measure this enhancement. Fermilab E906 will collect data using nuclear targets, in addition to hydrogen and deuterium to look for these effects.

From deep inelastic scattering (DIS) experiments, we know that the quark level structure of a nucleon with in a nucleus is different from that of a free nucleon. In the range $0.10 < x < 0.25$, a surplus of quarks (approximately 2-4%) in nuclei, known as antishadowing, is clearly observed in DIS data. To understand these phenomena, it is important to determine if it is a general property of the quark and antiquark distributions, or just a property of the valence or sea quarks. Drell-Yan, with its ability to measure sea-only quark effects, is the ideal reaction in which to measure this. Early Drell-Yan data indicate that this surplus might not be present,⁶ but with poor statistical uncertainty (3-5%). Fermilab E906's measurements

will clearly determine if there is antishadowing in the sea, with statistical uncertainties of less than 1% throughout this region (see Fig. V-15).

Using the same nuclear target data, Fermilab E906 will also study the propagation of colored partons in strongly interacting, cold nuclear matter. By comparing the Drell-Yan yields from different nuclear targets and looking for apparent shifts in the beam parton's momentum distributions between nuclei, E906 will be able to measure the beam parton's energy loss. Previous Drell-Yan studies have placed upper limits on parton energy loss.⁷ With increased sensitivity from the 120 GeV beam and better statistical accuracy, Fermilab E906 will turn these upper limits into measurements. These measurements will aid in the understanding of jet suppression data from RHIC.

FNAL E906 is able to make these improvements over previous measurements because of the lower beam energy available at the Fermilab Main Injector. For

fixed x_{beam} and x_{target} the cross section scales as the inverse of the beam energy. Thus a factor of seven more events for the same integrated luminosity can be achieved. At the same time, the primary background to the measurement, muons from J/ψ decays, decreases with decreasing beam energy, allowing for an increase in instantaneous luminosity by another factor of seven. These two factors combine to provide roughly 50 times more events for the same beam time.

FNAL E906 has been approved by the Fermilab PAC and will begin collecting data in 2009. Much of the new spectrometer will come from detector elements recycled from the E866 Drell-Yan spectrometer. To increase the rate and triggering capabilities of the spectrometer, some new detectors will be fabricated. In addition, because of the significantly different kinematics of the 120 GeV experiment, the new spectrometer will require a new, large dipole magnet to focus the Drell-Yan muons.

¹L. D. Isenhower *et al.* (Fermilab E906 Collaboration), "Proposal for Drell-Yan Measurements of Nucleon and Nuclear Structure with the FNAL Main Injector", April 1, 2001.

²E. A. Hawker *et al.* (Fermilab E866/NuSea Collaboration), Phys. Rev. Lett. **80**, 3715 (1998).

³R. S. Towell *et al.* (Fermilab E866/NuSea Collaboration), Phys. Rev. D **64**, 05202 (2001).

⁴M. J. Leitch *et al.* (Fermilab E866/NuSea Collaboration), Phys. Rev. Lett. **84**, 3256 (2000).

⁵J. C. Peng *et al.* (Fermilab E866/NuSea Collaboration), Phys. Rev. D **58**, 092004 (1998).

⁶D. M. Alde *et al.* Phys. Rev. Lett. **64**, 2479 (1990).

⁷M. A. Vasiliev *et al.* (Fermilab E866/NuSea Collaboration), Phys. Rev. Lett. **83**, 2304 (1999).

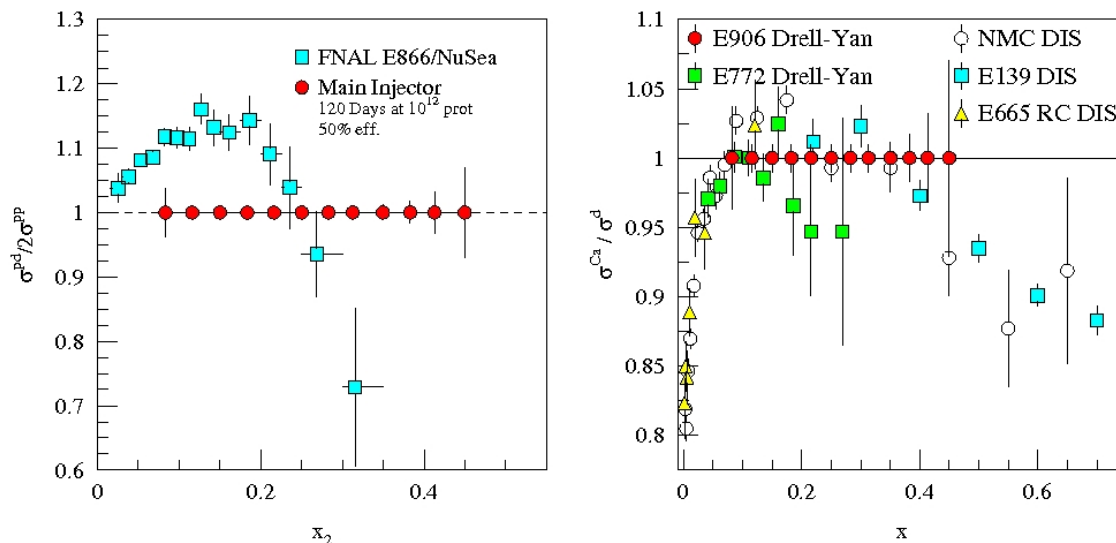


Fig. V-15. The statistical uncertainty of the proposed E906 measurement of the ratio of hydrogen to deuterium cross sections (arbitrarily plotted at 1) compared with the E866 measurements of the same quantity (left). The statistical uncertainty of E906's measurement of the ratio of deuterium to Calcium cross sections (arbitrarily plotted at 1) compared with previous Drell-Yan and deep inelastic scattering (DIS) measurements (right).

D. ATOM TRAP TRACE ANALYSIS

d.1. Laser Spectroscopic Determination^{1,2} of the Nuclear Charge Radius of ⁶He (L.-B. Wang,* P. Mueller, K. Bailey, J. P. Greene, D. Henderson, R. J. Holt, R. V. F. Janssens, C. L. Jiang, Z.-T. Lu, T. P. O'Connor, R. C. Pardo, K. E. Rehm, J. P. Schiffer, X. D. Tang, and G. W. F. Drake†)

The nucleus ⁶He, with 2 protons and 4 neutrons, has been intriguing for quite some time. Measurements in the eighties and nineties have indicated that, when used as a beam, the probability for it to induce a nuclear reaction on any target is much larger than that for ⁴He. This observation was interpreted as a strong indication that ⁶He is a three-body "halo" nucleus, *i.e.*, it can be best viewed as a tightly bound ⁴He core and two neutrons orbiting this core at large distances. Moreover, while these three constituents of ⁶He form a bound system, the nuclear potential is not strong enough to bind any two of them separately. For this reason, ⁶He is often referred to as "Borromean" (the name derives from the heraldic emblem of the medieval princes of Borromeo, three rings interlocked in such a way that the removal of any of the rings will cause the remaining two to fall apart).

Because of its intriguing properties, ⁶He has the potential to teach us about the fundamental forces among the constituent nucleons. Indeed, the halo character can be revealed by an accurate determination of the nuclear charge radius, since the motion of the core with regard to the center of mass reflects both the radial extent of the neutrons and the correlations between these particles. The result can in turn be compared with the most modern theories as recent advances in computational methods have made it possible to calculate the structure of few-nucleon systems from the basic interactions between the constituents.

The charge radius of ⁶He has been determined for the first time by measuring the atomic isotope shift between ⁶He and ⁴He using laser spectroscopy. For this work, ⁶He atoms were produced at the ATLAS accelerator facility at Argonne National Laboratory, and quickly captured and cooled by an on-line laser trap. By applying laser spectroscopy on the trapped ⁶He atoms as well as on their ⁴He isotopic partner atoms, the charge radius of the ⁶He nucleus was determined to be 2.054 ± 0.014 fm. The measurement is of such accuracy that it distinguishes between the available theoretical predictions. The data offer new insight into the dependence of three-body interactions on neutron number, which in turn is essential to the understanding of the structure of all neutron-rich systems, including neutron stars.

In this work, ⁶He nuclei were produced via the ¹²C(⁷Li, ⁶He)¹³N reaction with a 100 pA, 60 MeV beam of ⁷Li from the ATLAS accelerator at Argonne National Laboratory. Neutral ⁶He atoms diffused out of the hot graphite target and were transferred in vacuum to the nearby atomic beam assembly at a rate of approximately 1×10^6 s⁻¹. Trapping helium atoms in the 2³S₁ metastable level was accomplished by exciting the 2³S₁ – 2³P₂ transition using laser light with a wavelength of 1083 nm. ⁶He atoms were mixed with a krypton carrier gas and sent through a discharge to be excited to the 2³S₁ level. The metastable ⁶He atoms were transversely cooled, decelerated with the Zeeman slowing technique, and then captured in a magneto-optical trap at a rate of approximately one atom per minute.

*University of Illinois-Urbana, †University of Windsor, Ontario.

¹Project homepage: <http://www-mep.phy.anl.gov/atta/>.

²L.-B. Wang *et al.*, Phys. Rev. Lett. **93**, 142501 (2004).

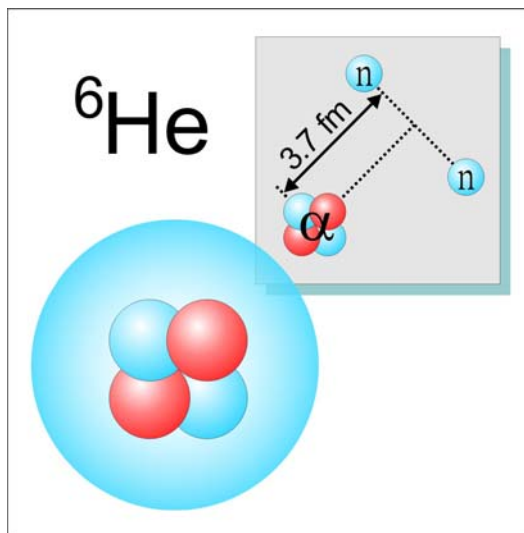


Fig. IV-16. Halo nucleus ${}^6\text{He}$. The nucleus can be viewed as a three-body cluster consisting of a particle core and two loosely bound neutrons.

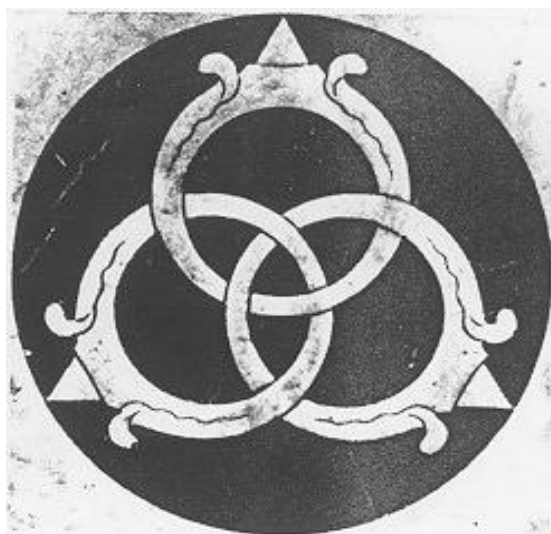


Fig. IV-17. Borromean rings.

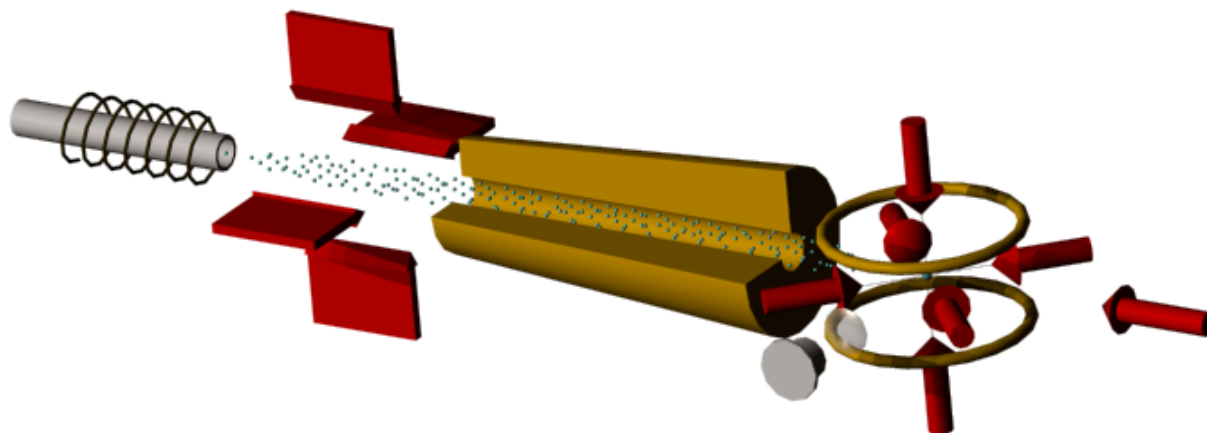


Fig. IV-18. Atomic beam apparatus for the laser trapping and laser spectroscopy of ${}^6\text{He}$ atoms.

d.2. Fine Structure of the $1s3p\ ^3P_J$ Level in Atomic ^4He : Theory and Experiment (P. Mueller, L.-B. Wang,* K. Bailey, Z.-T. Lu, T. P. O'Connor, and G. W. F. Drake†)

The fine structure intervals in helium have attracted a great deal of interest in recent years because of the possibility of using a comparison between theory and experiment to better determine the fine structure constant α . We report on a theoretical calculation and a new experimental determination of the $1s3p\ ^3P_J$ fine structure intervals in atomic ^4He . The values from the theoretical calculation of 8113.730(6) MHz and 658.801(6) MHz for the ν_{01} and ν_{12} intervals, respectively, disagree significantly with the previous most precise experimental results. However, the new

laser spectroscopic measurement¹ reported here yields values of 8113.714(28) MHz and 658.810(18) MHz for these intervals. These results² show an excellent agreement with the theoretical values and resolve the apparent discrepancy between theory and experiment.

This measurement was performed using the apparatus of the ^6He project. In addition to the aforementioned motivation, the measurement also serves as an important test and calibration of the apparatus for the ^6He project.

*University of Illinois-Urbana, †University of Windsor, Ontario.

¹Project homepage: <http://www-mep.phy.anl.gov/atta/>.

²P. Mueller *et al.*, Phys. Rev. Lett. **94**, 133001 (2005).

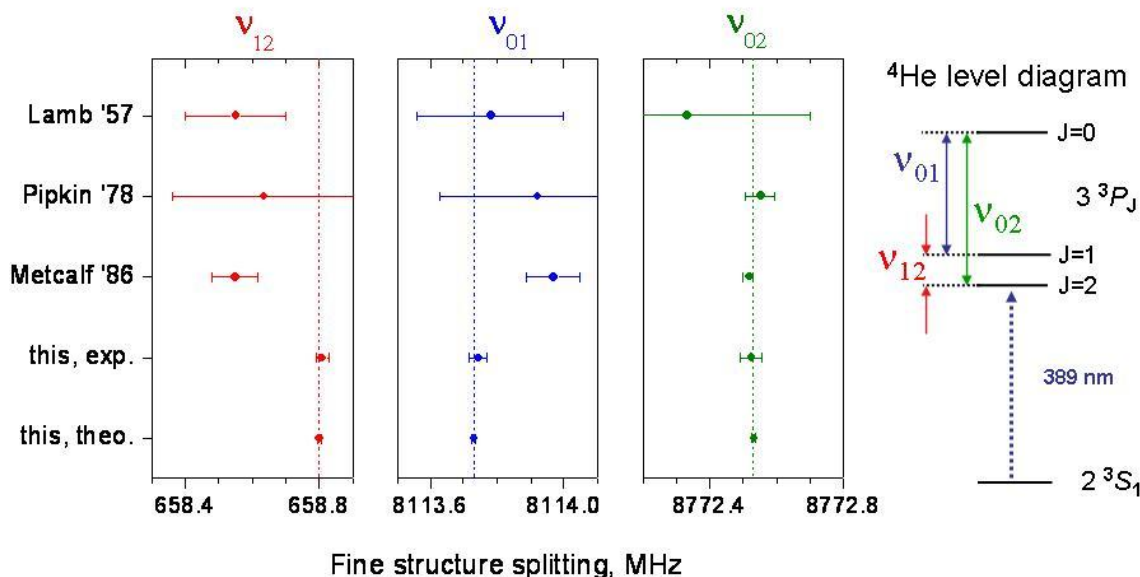


Fig. IV-19. Comparison of results for the three fine structure intervals of the $1s3p\ ^3P_J$ levels.

d.3. Atmospheric ^{81}Kr as an Integrator of Cosmic Ray Flux Over the Past $\sim 3 \times 10^5$ Years¹ (Z.-T. Lu, P. Mueller, T. P. O'Connor, L.-B. Wang, R. Purtschert,* J. Elsig,* B. M. Kennedy,† N. C. Sturchio,‡ and G. Wolber§)

The variability of the cosmic ray flux over time can be studied based on the measurements of a variety of radionuclides. The flux is known to correlate with the short-term (~ 10 year) solar cycles and with the long-term ($\sim 10^4$ year) variations of geomagnetic fields. The atmospheric ^{81}Kr is an ideal integrator of the cosmic ray flux over the ^{81}Kr lifetime of 3.3×10^5 years. ^{81}Kr is

produced by cosmic-ray induced spallation and nuclear reaction of stable Kr nuclei in the atmosphere. Once produced, over 98% of ^{81}Kr remain in the atmosphere with its radioactive decay as its only sink. Based on the abundance of ^{81}Kr in the atmosphere, the cosmic ray flux integrated over the past 3×10^5 years can be

calculated with models that simulate the production of cosmogenic radionuclides.

This collaboration aims to accurately determine the isotopic abundance of ^{81}Kr in the atmosphere. Enriched samples of ^{81}Kr and ^{85}Kr are analyzed with Mass Spectrometry (MS), Low-Level Counting (LLC), and

Atom Trap Trace Analysis (ATTA). Once ATTA is calibrated against MS for $^{81}\text{Kr}/^{85}\text{Kr}$ ratios, ATTA can be used to measure the absolute isotopic abundance of ^{81}Kr in the Earth's atmosphere. At present, calibration measurements and investigation of various systematic effects are in progress.

*University of Bern, Switzerland, †Lawrence Berkeley National Laboratory, ‡University of Illinois-Chicago,

§Deutsches Krebsforschungszentrum Heidelberg, Germany.

¹Project homepage: <http://www-mep.phy.anl.gov/atta/>.

E. FUNDAMENTAL SYMMETRIES IN NUCLEI

e.1. Probing the Intercombination Transition $7s^2\ ^1S_0 - 7p\ ^3P_1$ in ^{225}Ra Atoms for an EDM Measurement (N. D. Scielzo, J. R. Guest, E. C. Schulte, I. Ahmad, K. Bailey, J. P. Greene, R. J. Holt, Z.-T. Lu, T. P. O'Connor, and D. H. Potterveld)

The goal of this project is to measure the electric dipole moment (EDM) of the ^{225}Ra atom. ^{225}Ra is an especially good case because it has a relatively long lifetime, has spin $\frac{1}{2}$ that eliminates systematic effects due to electric quadrupole moments, is available in relatively large quantities from the decay of ^{229}Th , can be trapped with readily available lasers, and has a well-established octupole nature. The octupole deformation enhances the signal from an atomic EDM by increasing the Schiff moment collectively and by the parity doubling of the energy levels. The overall scheme is to collect ^{225}Ra atoms in a magneto-optical trap and transfer the sample to an optical dipole trap. In this second trap, the atoms will be polarized by optical pumping and the EDM measurement will be performed.

We have recently characterized the intercombination transition $7s^2\ ^1S_0 - 7p\ ^3P_1$ on which laser manipulation

of neutral ^{225}Ra atoms will be developed. We obtained 10^8 ^{225}Ra atoms/sec from the oven at temperatures of ~ 700 C by adding barium metal to the existing oven setup to aid in the chemical reduction. By performing laser induced fluorescence measurements on this atomic beam of ^{225}Ra , we have determined the frequency of the transition to the $F = 3/2$ excited state to be $13999.27\ \text{cm}^{-1}$. This frequency is ≈ 710 MHz from a transition in molecular iodine (line number 692 of the I_2 atlas), which we use to control the laser frequency. We have also determined the lifetime of the $7p\ ^3P_1$ state to be 422 ± 20 ns, and derived the strength of the intercombination line. Therefore, the maximum acceleration that can be applied by photon scattering using this transition is $2.9\ \text{km/s}^2$. A magneto-optical trap for ^{225}Ra atoms based on this transition is under development.

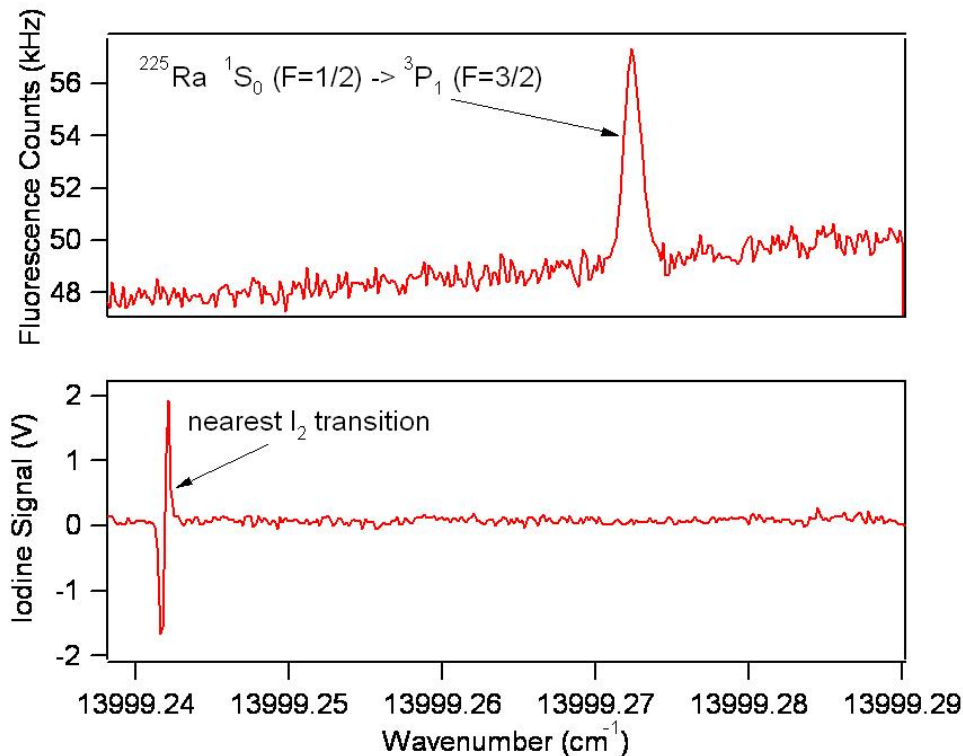


Fig. IV-20. Laser induced fluorescence signal of neutral ^{225}Ra atoms. The laser frequency is scanned across the intercombination transition $7s^2\ ^1S_0 - 7p\ ^3P_1$. The iodine transition shown is used to control the laser frequency.

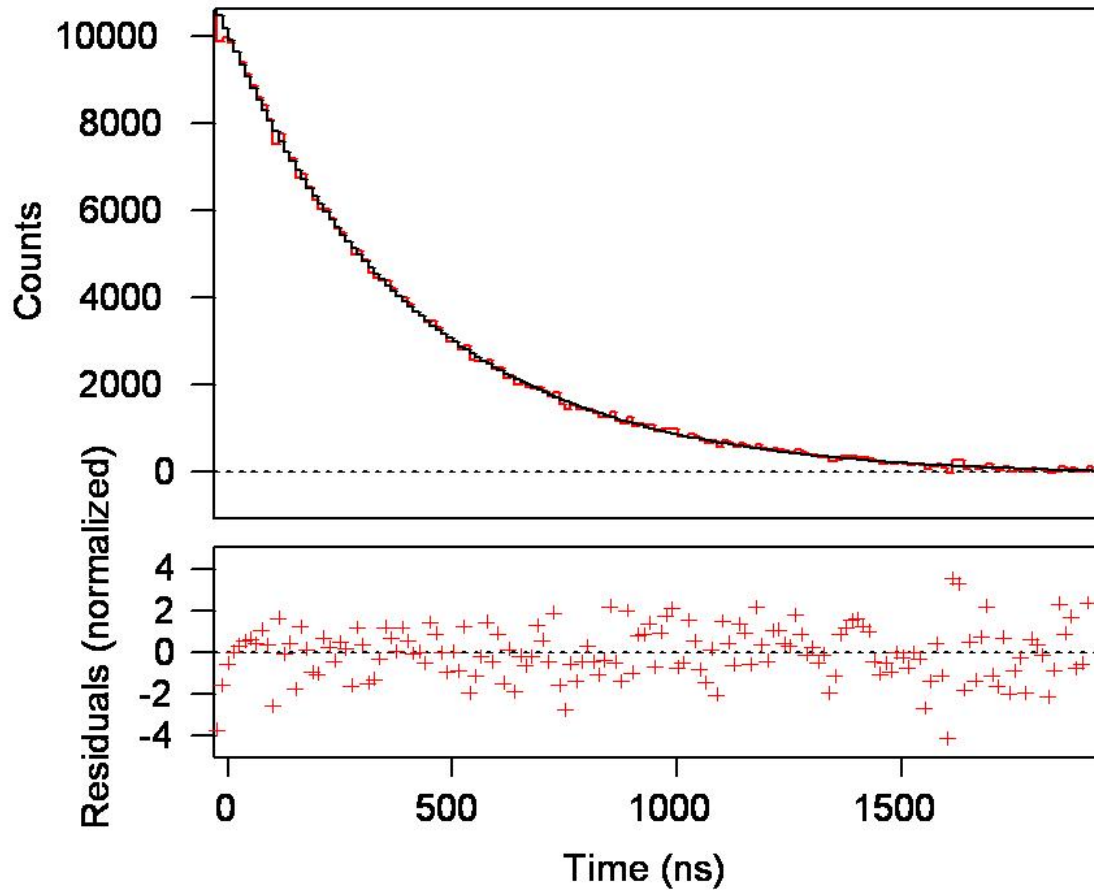


Fig. IV-21. The decay of the fluorescence signal of neutral ^{225}Ra atoms after turning off of the excitation laser pulse at time = 0. Lifetime of the $7p\ ^3P_1$ state is 422 ± 20 ns.

e.2. Measurement of $\sin^2 \theta_W$ Through Parity Violation in Deep Inelastic Scattering (PV DIS) on Deuterium (P. E. Reimer, X. Zheng, J. Arrington, K. Hafidi, R. J. Holt, H. E. Jackson, and D. H. Potterveld)

One of the basic parameters of the Standard Model is $\sin^2 \theta_W$, which represents the relative coupling strength of the weak and electromagnetic forces. The Standard Model predicts that the value $\sin^2 \theta_W$ will vary (or run) as a function of Q^2 , the energy squared at which it is probed. Measurement of this “running” provides a strict test of the Standard Model. At an energy equivalent to the mass of the Z-boson ($Q^2 = M_Z^2$), $\sin^2 \theta_W$ is well measured; but at $Q^2 < M_Z^2$, only a few measurements exist. The asymmetry from parity violation in polarized electron-deuterium deep inelastic scattering (DIS) is linearly dependent on $\sin^2 \theta_W$ and relatively large ($A_d \approx 10^{-4} Q^2$), making it experimentally quite accessible. The sensitivity to $\sin^2 \theta_W$ is through the product of the axial Z-electron

and vector Z-quark couplings (C_{1q}) and the product of the vector Z-electron and axial Z-quark couplings (C_{2q}). Historically, DIS parity violation from a deuterium target was first observed by Prescott *et al.* at SLAC in the mid-1970 and was used to establish the Weinberg-Salam model. Investigations are underway to repeat this experiment with much better precision, focusing on facilities at an upgraded 12 GeV JLab.¹

A preliminary measurement at JLab with a 6 GeV beam has been approved (E05-007).² The 6 GeV measurement will, when combined with other data, provide a measurement of $(2C_{2u} - C_{2d})$. Current experimental knowledge of this quantity has an uncertainty of 300%. The complete measurement at 6 GeV will reduce this

uncertainty by a factor of eight as shown in Fig. IV-22. In addition, the 6 GeV experiment will explore the contribution of higher-twist effects to the

asymmetry, providing crucial guidance to interpreting this data and future PV-DIS measurement with the 12 GeV upgrade to JLab.

¹Conceptual Design Report for the 12 GeV Upgrade of CEBAF, J. Arrington *et al.*, eds., JLab, February 2005.

²J. Arrington *et al.*, " \bar{e} - ^2H Parity Violating Deep Inelastic Scattering at CEBAF 6 GeV", proposal 05007 to the JLab PAC, P. E. Reimer and X. Zheng, spokespersons, December 6, 2004.

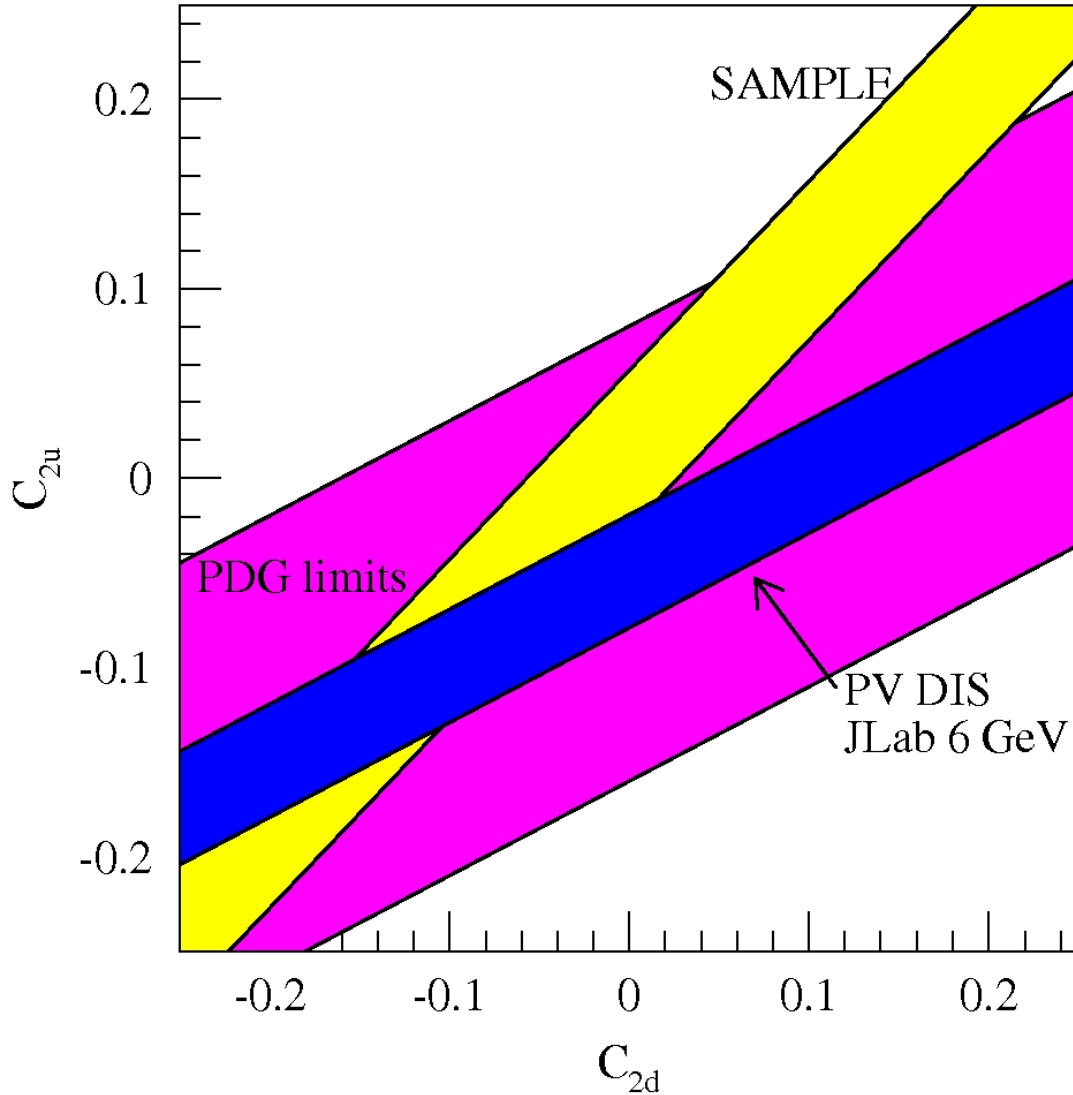


Fig. IV-22. Plot of C_{2u} vs. C_{2d} showing the current Particle Data Group (PDG) limits. The blue band shows the improvement which will be achieved by the 6 GeV JLab experiment. The yellow band represents constraints on C_{2u} and C_{2d} from the SAMPLE experiment.

e.3. Feasibility Study for a Charge Symmetry Violating Quark Distribution

Measurement (K. Hafidi, J. Arrington, A. El Alaoui, L. El Fassi, D. F. Geesaman, R. J. Holt, H. E. Jackson, B. Mustapha, D. Potterveld, P. E. Reimer, E. C. Schulte, and X. Zheng)

Symmetries are the key to understanding and classifying the structure of matter and the fundamental forces and their study leads to better understanding of the underlying physics. Therefore, it is important to test fundamental symmetries, even the approximate ones such as Isospin (IS) and Charge (CS) symmetries. IS requires invariance under all rotations in isospin space such that the Hamiltonian of the system commutes with the isospin operator while CS is related to only one rotation. It requires invariance with respect to rotations of 180° about the T_2 axis, where the charge corresponds to the third axis. If CS is a valid symmetry the Hamiltonian has to commute with the charge symmetry operator.

At the quark level, CS implies the invariance of a system under the interchange of up and down quarks while simultaneously interchanging protons and neutrons, *i.e.*,

$$u^p(x, Q^2) = d^n(x, Q^2) \text{ and } d^p(x, Q^2) = u^n(x, Q^2)$$

Quantum Chromo-Dynamics (QCD) provides a clear formulation of the origin of Charge Symmetry Violation (CSV). In QCD, the only sources of CSV are electromagnetic interactions and the mass difference $\delta m = m_d - m_u$ between down and up quarks. Electromagnetic interactions should play a minor role at high energies. Thus the light quark mass difference is the interesting feature of the QCD view of CSV.¹ CS is a more restricted symmetry than IS; therefore it is generally conserved in strong interactions to a greater degree than IS.² In fact, while in many nuclear reactions IS is violated at the few percent level, in most cases CS is obeyed to better than one percent: the proton and neutron masses are equal to about 1%; the binding energies of tritium and ^3He are equal to 1%, after Coulomb corrections. By comparing energy levels in mirror nuclei, one generally finds agreement to better than 1%, correcting for electromagnetic interactions. At the parton level, one would naively expect CSV to be of the order of up-down current mass difference divided by some average mass expectation value of the strong Hamiltonian which has a value roughly 0.5-1.0 GeV. This would put CSV effects at a level of 1% or smaller.³ From our experience with CS in nuclear systems, and because of the order of

magnitudes estimates of CSV in parton systems, CS has been universally assumed in quark distribution functions. CS reduces by a factor of two the number of independent quark distributions necessary to describe high-energy data, and until recently there has been no compelling reason to suggest CSV. On the other hand, there were no precise tests of charge symmetry in parton distributions. Recently much attention has been focused on the apparent violation of what is called SU(2) flavor symmetry in the nucleon. This was suggested by New Muon Collaboration (NMC)⁴ and later supported by results from NA51 group at CERN⁵ and E866 Drell-Yan experiment⁶ at FNAL. Experimental results from these collaborations seem to show a large flavor symmetry violation in the proton sea distributions. However this could also in principle be explained even if flavor symmetry were conserved, if we assume very large CSV in the nucleon sea. The valence quark CSV is also very important issue because it makes a substantially larger contribution than the sea quark CSV to the extraction of the Weinberg angle from neutrino Deep Inelastic Scattering (DIS). The three standard deviation result from the Standard Model prediction reported by NuTeV collaboration⁷ or the so-called ‘‘NuTeV anomaly’’ could be completely removed by assuming valence quark CSV without being in conflict with high energy data.⁸

At present, there are no direct measurements that reveal the presence of CSV in parton distribution functions. We have only upper limits on its magnitude. These limits arise from comparing the structure function measured in neutrino induced charged current reactions, and the one for charged lepton DIS, both measurements on isoscalar targets. In the region of $0.1 \leq x \leq 0.4$, an upper limit of 9% was set for CSV effects.

Semi-inclusive pion production from lepton DIS on nuclear targets was suggested³ as a sensitive probe of CSV effects in nucleon valence distributions. The authors proposed measuring the quantity $R_{\text{meas}}(x, z)$ defined by:

$$R_{\text{meas}}(x, z) = \frac{4N^{D\pi^+}(x, z) N^{D\pi^+}(x, z)}{N^{D\pi^+}(x, z) N^{D\pi^-}(x, z)}$$

Where $N^{D\pi^+}$ ($N^{D\pi^-}$) is the yield of π^+ (π^-) produced in coincidence with the scattered electron from deuterium.

In the quark-parton formalism, the yield of hadron h per scattering from nucleon N can be written as

$$N^{Nh} = \sum_i e_i^2 q_i^N(x) D_i^h(z).$$

The quantity $q_i^N(x)$ is the distribution functions for quarks of flavor i , and charge e_i , in the nucleon N as a function of Bjorken x . $D_i^h(z)$ is the fragmentation function for a quark of flavor i into hadron h . It

$$R(x, z) = \frac{1 - \Delta(z)}{1 + \Delta(z)} R_{\text{meas}}(x, z), \text{ and } \Delta(z) = \frac{D_u^{\pi^-}(z)}{D_u^{\pi^+}(z)}$$

$$R_f(z) = \frac{5\Delta(z)}{1 + \Delta(z)} - \frac{[4 + \Delta(z)]\delta D(z)}{3[1 - \Delta^2(z)]}, \text{ and } \delta D(z) = \frac{D_u^{\pi^+}(z) - D_d^{\pi^-}(z)}{D_u^{\pi^+}(z)}$$

$$R_{\text{CSV}}(x) = \frac{4[\delta d(x) - \delta u(x)]}{3[u_V^p(x) + d_V^p(x)]}, \delta d(x) = d^p(x) - u^n(x), \delta u(x) = u^p(x) - d^n(x)$$

$$R_{\text{sea}}(x, z) = \frac{5[u_V^{-p}(x) + d_V^{-p}(x)] + \Delta_S(z)[s(x) + \bar{s}(x)]/[1 + \Delta(z)]}{[u_V^p(x) + d_V^p(x)]}, \text{ and } \Delta_S(z) = \frac{D_S^{\pi^+}(z) + D_S^{\pi^-}(z)}{D_u^{\pi^+}(z)}$$

Experimentally, one needs to measure accurately the x dependence of $R(x, z)$ for fixed z values. The sea quark distribution $R_{\text{sea}}(x, z)$ should fall off monotonically and rapidly with x . Therefore by going to sufficiently large x region, the sea contribution will be negligible relative to the CSV term. The CSV contribution of the fragmentation function to the z -dependent term $R_f(x, z)$ was estimated⁹ to be 1%. Therefore it can also be neglected. Because of the low DIS cross sections at high x , these measurements would not be possible

depends on the quark longitudinal momentum fraction $z = E_h/\nu$, where E_h is the energy of the hadron and ν is the energy of the virtual photon. Assuming the validity of the impulse approximation and multiplying R_{meas} by a z -dependent factor, one obtains the following expression;

$$R(x, z) = R_f(z) + R_{\text{CSV}}(x) + R_{\text{sea}}(x, z)$$

where

without the high luminosity available at JLab. Studies have shown that Hall C would be the best place to perform these measurements. Figure IV-23 shows the projected uncertainties of $[\delta d(x) - \delta u(x)]$ with 30 days of data taking using Hall C spectrometers HMS and SOS, 4 cm LH₂ target and 50 μ A electron beam at 6 GeV. Systematic errors related to the detectors efficiencies and particle identification are taken into account. More studies concerning the validity of factorization and contributions from high mass resonances to the pion yield are underway.

¹G. A. Miller, Nucl. Phys. **A518**, 345 (1990); I. Slaus, B. M. K. Nefkens, and G. A. Miller, Nucl. Instrum. Methods **B56/57**, 489 (1991).

²E. M. Henley and G. A. Miller in *Mesons in Nuclei*, eds., M. Rho and D. H. Wilkinson (North-Holland, Amsterdam 1979).

³J. T. Londergan and A. W. Thomas, Prog. Part. Nucl. Phys. **41**, 49 (1998).

⁴P. Amaudruz *et al.*, (NMC Collaboration), Phys. Rev. Lett. **66**, 2712 (1991), Phys. Lett. **B295**, 159 (1992).

⁵A. Baldit *et al.* (NA51 Collaboration), Phys. Lett. **B332**, 244 (1994).

⁶E. A. Hawker *et al.* (E866 Collaboration), Phys. Rev. Lett. **80**, 3715 (1998), R. S. Towell *et al.*, Phys. Rev. D **64**, 052002 (2001).

⁷G. P. Zeller *et al.* (NuTeV Collaboration), Phys. Rev. Lett. **88**, 091802 (2002).

⁸A. D. Martin, R. G. Roberts, W. J. Stirling, and R. S. Thome, hep-ph/0308087.

⁹J. T. Londergan, A. Pang, and A. W. Thomas, Phys. Rev. D **54**, 3154 (1996).

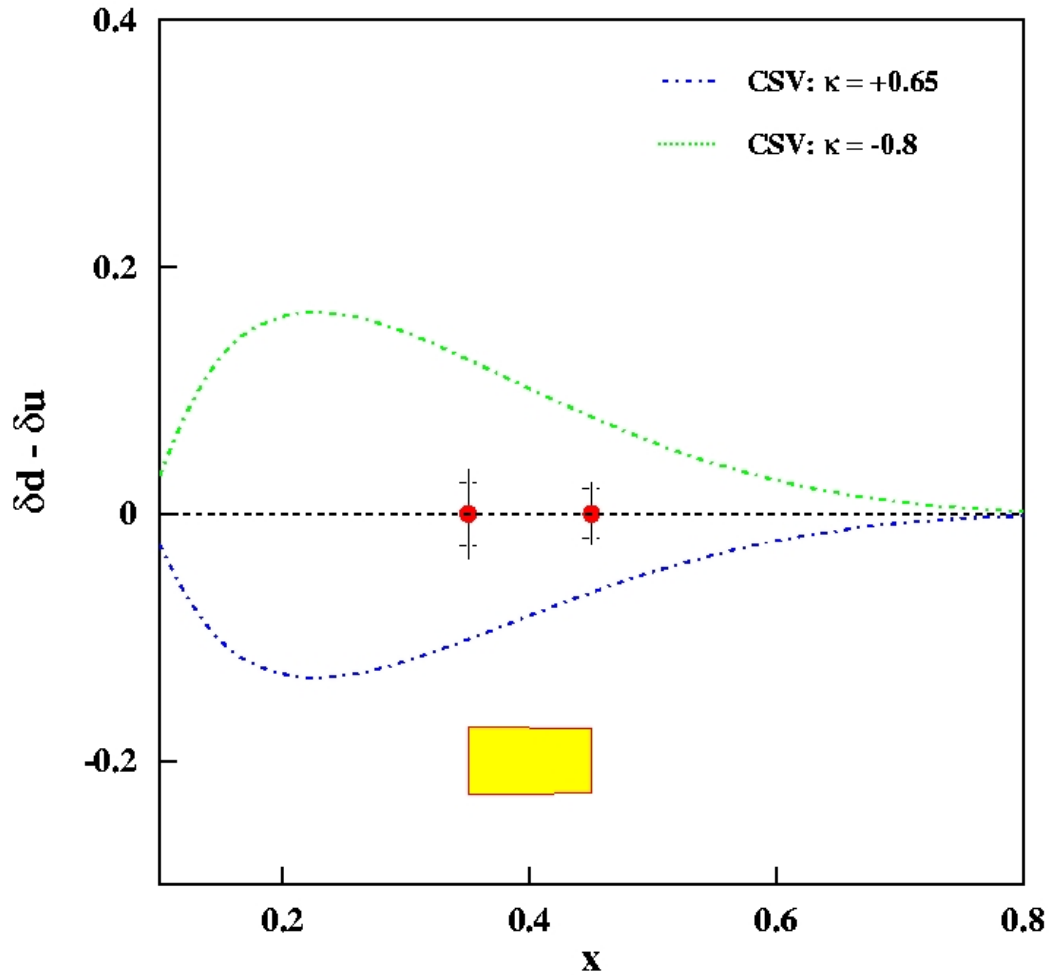


Fig. IV-23. The two curves are the upper and lower limit of CSV contribution given by MRST parameterization. Both statistical and systematical errors are included. The yellow band corresponds to the systematic error related to our present knowledge of PDFs.